

Evaluation of the RCIC for Extended Operation

TEAM 11

Homer, Michael

Leighton, Jacob

Banuelos, Cervando

Technical Advisor

Professor Karen Vierow

NUEN 410 Senior Design Project

Final Report

Nuclear Engineering Department

Texas A&M University

College Station, TX 77843-3133

April 30, 2013

Evaluation of the RCIC for Extended Operation

TEAM 11

Homer, Michael

Leighton, Jacob

Banuelos, Cervando

Technical Advisor

Professor Karen Vierow

NUEN 410 Senior Design Project

Final Report

Nuclear Engineering Department

Texas A&M University

College Station, TX 77843-3133

April 30, 2013

<u>Contents</u>	<u>Page</u>
EXECUTIVE SUMMARY (Michael, Cervando)	(i)
I. INTRODUCTION	(1)
A. NEUTRONICS (Cervando)	
B. THERMAL HYDRAULICS (Michael)	
C. SYSTEM MODIFICATIONS (Jacob)	
II. OBJECTIVES	(3)
A. NEUTRONICS (Cervando)	
B. THERMAL HYDRAULICS (Michael)	
C. SYSTEM MODIFICATIONS (Jacob)	
III. APPROACH	(5)
A. NEUTRONICS (Cervando)	
1. Theory and Relevant Equations	
2. Background Research	
3. Methodology	
B. THERMAL HYDRAULICS (Michael)	
C. SYSTEM MODIFICATIONS (Jacob)	
IV. DISCUSSION	(24)
A. NEUTRONICS (Cervando)	
1. Hand Calculations for Decay Heat Approximation	
2. ORIGEN-ARP Decay Heat Simulation	
3. ORIGEN-ARP Results vs. Decay Heat Estimates	
B. THERMAL HYDRAULICS (Michael)	
C. SYSTEM MODIFICATIONS (Jacob)	
V. CONCLUSIONS	(46)
A. NEUTRONICS (Cervando)	
B. THERMAL HYDRAULICS (Michael)	
C. SYSTEM MODIFICATIONS (Jacob)	
REFERENCES	(50)
APPENDIX Input Decks, Data (Michael, Cervando)	(52)

EXECUTIVE SUMMARY

The Reactor Containment Isolation Cooling System (RCIC) is a safety system for Boiling Water Reactors (BWR) that is intended to be used for cooling the core during reactor isolation. The system is currently thought of as being capable of operating for at most 12 hours; actual capabilities are very site specific. However, it was seen in the unfortunate events of the Fukushima Daiichi disaster that the system functioned for much longer than previously anticipated. The intention of this project is to show that the RCIC system found in BWRs currently in use today, or the system with slight upgrades, can be relied on for longer than the industry held 12 hours.^[1]

Since there are multiple reasons why the RCIC may fail the scope of this analysis will focus on the heat generated within the room where the system is located. This was done by first modeling the neutronics of the core to determine the amount of heat that continues to be produced once it is shutdown. The current configuration of the RCIC system was then used to do a thermal hydraulic analysis of the system. The thermal hydraulics results were then used to determine the rate at which the room will increase in temperature. Once the heat generation rate within the room was known, a heat exchanger and water driven fan were designed to dissipate the heat from the room. The flow for the heat exchanger and propulsion for the fan was required to come from the RCIC pump since the system is intended to be used during a station blackout. Thus, an optimization of the flow requirements of the heat exchanger and the flow needed for the reactor was performed to ensure a balance between the two.

The RCIC system removes the decay heat generated in the core after an emergency scram and in order to effectively model the RCIC under operational conditions required data from a reactor core under station blackout conditions. This was done by modeling a boiling water reactor (BWR) core for up to 72 hours immediately following a reactor scram. The modeling was done in two different ways. One way was done using a hand equation that gives an estimate of decay heat of up to 100 hours after power-down, regardless of reactor type, enrichment, or fuel layout. The second approach was made with the ORIGEN-ARP module of the SCALE6.1.2 Suite, which allowed the modeling of the total decay heat and isotope production throughout a BWR core after a specified burnup and period of operation. This simulation was also designed to produce viable results that could be comparable to the decay heat generated by the BWR at the Fukushima Daiichi site during and immediately following the disaster of 2011. To best approximate the BWR unit at the Fukushima Daiichi site, the model had to be based on a similar BWR system that also had a corresponding RCIC system. The reactor chosen was the BWR at the Monticello Nuclear Generating Plant. Using its core and fuel specifications, a decay heat model for a core that had been at full power for 365 days was generated with a decay time of 72 hours. In order to validate this deck, the output plot was compared to that of the estimate done by hand and plotted the data trends to see if the results were within acceptable limits. The data was found to fit the curve of the estimate within realistic limits, and therefore was a viable input to the thermal hydraulics analysis of the heat removal provided by the RCIC system. With the decay heat known it was then possible to model the system in RELAP5. The RELAP5 code is an industry used thermal hydraulics code that allowed for an analysis of how the system as a whole functions.

An analysis of the heat emitted from the turbine will be conducted in order to design a heat exchanger to prevent the overheating of the turbine's containment room. A heat exchanger design software produced by KamLex will be used to aide in the design. Hand calculations will be used to verify the validity of the software as it is not industry standard.

Finally, an economic analysis of the RCIC modifications was performed to determine the financial impact to the plants. It was found that with respect to the amount of money generated by the plants on a daily basis, the costs of implementing the design changes were very minimal.

It was found that with addition of the heat removal system, the RCIC is capable to run for at least 19 hours. This is a significant improvement over the previously held belief of between 4 and 12 hours. It is likely that with future research and design, the RCIC system could be expected to operate for three days which would provide a significant contribution to the safety of a BWR.

I. INTRODUCTION

The main purpose of the RCIC system is to provide makeup water to the core when the core is isolated from the turbine-condenser. The heart of the system consists of a steam-driven turbine-pump unit. The turbine-pump unit is turned on automatically under the following three main conditions:

- complete shutdown with the loss of normal feedwater before the reactor is depressurized to a level where the shutdown cooling system can be placed in operation
- the reactor pressure vessel has been isolated and maintained at hot standby
- a loss of AC power

The system is designed to provide enough coolant to keep up with the decay heat from the reactor. Since the decay heat reduces rapidly after a reactor scram, the RCIC system will quickly have extra cooling capacity.^[1]

After the Fukushima Daiichi disaster, the RCIC system ran for 72 hours. This led to the question of what factors enabled the operation of the system past the expected time limit and also if the system can be modified so that it can be relied upon for longer periods of time. Since there are multiple causes of failure in the RCIC system only one failure mode will be explored and the rest will be left up to further research and study to determine the full capabilities and design changes of the system.

There are currently 31 nuclear power plants in the United States that have the RCIC system as a safety feature. If it is shown that the system itself or a slightly modified system can

operate for a longer length of time, it will increase the inherent safety of the 31 nuclear power plants.

I.A. NEUTRONICS

To incorporate a neutronics analysis into the RCIC system meant that a realistic core had to be modeled. This model was required to produce real results from a BWR, and provide the decay heat data from a real and verified isotopics library. For these reasons, the ORIGEN-ARP module of the SCALE 6.1 suite was selected as the software and code of choice. This code allows for the calculations based on input parameters of a real BWR and provides an output of the decay heat as a function of time for the radioactive isotopes produced during normal operation in the modeled core. These decay heat outputs were then given to the thermal hydraulic section where the RCIC was modeled.

I.B. THERMAL HYDRAULICS

To do the thermal hydraulic analysis, RELAP5 was chosen to do the modeling of the system. The specific version used was RELAP5-3D/Ver:1999cf02Reactor Loss Of Coolant Analysis Program. This code was chosen because it is an industry trusted thermal hydraulics simulation code. It allows for the modeling of the coupled behavior of the reactor coolant system during various transients and accidents. The code will allow for the system to trip on and off which will simulate the RCIC system being turned on and off with respect to the volume of coolant in the reactor. With the decay heat results from the neutronics analysis, heat structures were used to model the decay heat in the RELAP5 input deck. With the results of the thermal hydraulics analysis, it was then possible to design a heat removal system to ensure that the RCIC stays within operating parameters

I.C. SYSTEM MODIFICATIONS

The entire purpose of our project is to determine the length of operation of the RCIC system and extend that operation time to 19 plus hours as cheaply and as effectively as possible. There are many reasons why the RCIC system would fail, with some reasons being easier, or much more difficult, to handle than others. One reason was the system would run out of DC power from the batteries that are stored on-site to power the system. This problem is a simple fix by simply installing larger, or more of the same size, batteries. This would allow the system to operate without the potential for running out of power. However, this addition to the system is miniscule. The rate of failure due solely to the batteries running out of energy is small, so the focus was shifted to another main problem the system has when undergoing long term operation. During operation, the turbine that drives the pump that feeds water into the core for cooling tends to heat up the room that it is contained in. Over time, the turbine heats the room to such a temperature that the safety temperature switches trip, preventing the safe operation of the turbine. An obvious solution to this problem would be to design a heat exchanger that would incorporate well into the systems already present and working in the reactor.

II. OBJECTIVES

II.A. NEUTRONICS

The main objective of the neutronics portion of this project was to effectively model the decay heat of a BWR core for up to 72 hours after an emergency reactor scram. This scenario is of particular interest because of the events that transpired at the Fukushima Daiichi plant in 2011 where the RCIC system ran longer than its rated 12 hours.^[2] In order

to satisfy this objective, the data and specifications of the reactor core from the Monticello Nuclear Generating Plant were used. This plant was chosen because it is of a similar core and containment build as the Fukushima Daiichi reactor of interest, because it has an RCIC system, and because its technical specifications were readily available and accessible to us.^[3] The data provided from this model was used by the Thermal Hydraulics portion in order to determine and model the behavior of the RCIC pump and turbine, and by the structural analysis portion to do stress and strain analysis on the system. Minor objectives of the neutronics portion of this project included an analysis of the populations of several isotopes within the core as a function of decay time and hand calculations to estimate decay heat knowing basic parameters without isotopic data. These minor objectives were mostly used to ensure that the generated model agreed with modern nuclear reactor theory.

II.B. THERMAL HYDRAULICS

The primary objective of this project is to calculate if the RCIC system, with as few modifications as possible, can be expected to operate for 19 hours. The threshold of 19 hours was chosen because it was determined that the condensate storage tank holds enough coolant to cool the core during this period of time.^[4] To achieve this objective it was required to use the modeling of the decay heat of the core in the modeling of the thermal hydraulics. Also, since modifications were made to the system to cool the room that contains the RCIC system, a second model was made to determine if the condensate storage tank had enough inventory to cool the core while also providing coolant to the heat exchanger. With this data it will be shown that the RCIC system and condensate storage tank can be relied upon for at least 19 hours.

II.C. SYSTEM MODIFICATIONS

The objective of this portion of the project is to design a heat exchanger that would allow the most cost effective means to remove heat from the turbine containment, allowing a longer operation time of the turbine. The numerical goal that was chosen was a reliability of the RCIC system for at least 19 hours. In order to achieve this, reasons why the RCIC fails needed to be examined to determine the most effective way to design something that would extend the reliable life of the system. Several things were examined: the temperature of the room containing the turbine, the lifetime of the batteries used to power the switches and controllers in the system, over-filling of the core, and the temperature of the suppression pool. Each of these is a significant problem that needs to be dealt with, however, with the limited time given for this project, only the heat of the room was analyzed in detail. It is desirable to design an addition to the system that would be both effective at extending the reliability of the system as well as cost effective, including manufacturing and cost of integration.

III. APPROACH

III.A. NEUTRONICS

III.A.1 Theory and Relevant Equations

The heat (both operational and decay) generated by a nuclear reactor can be explained by modern reactor kinetics theory. This theory introduces several neutron and isotope balance equations where the behavior of the population is described over a defined period of time. These equations relate to the power in the reactor since it is the neutron population in the

core what determines the fission rate in the core and thus the power output of the core. To establish a fundamental understanding of the neutronics involved with the project, the reactor kinetics equation that took into account delayed neutron sources was explored. It was concluded these equations would be the most relevant to understanding the core model for several reasons. The first reason was that the model core was going to be fully operational for 365 days at full power before the scram event, which would allow for the understanding of the neutron and isotope population production as a function of operational time. The second reason was that this equation took into account the production of the delayed neutron precursors. These precursors do not produce neutrons from prompt fission, but rather by radioactive decay and are divided into 6 major groups. In the event of a scram when all of the prompt neutrons are absorbed by the control rods, decay heat is generated from the fission of fuel by these delayed neutrons.^[5] Below are the corresponding reactor kinetics equations that best modeled our reactor core. The final equation is shown below in Eqs. (7a) and (7b).

$$\frac{d}{dt}n(t) = \#prompt\ neutrons\ produced + \#delayed\ neutrons\ produced \quad (1)$$

$$\frac{d}{dt}C_i(t) = \#of\ precursors\ produced - \#of\ precursors\ decaying \quad (2)$$

$$\rho = \frac{k-1}{k} \quad (3)$$

$$\beta = \sum_{i=1}^6 \beta_i \quad (4)$$

$$\Lambda = \frac{1}{k} \quad (5)$$

$$\lambda_i = \frac{\ln(2)}{t_{i\ 1/2}} \quad (6)$$

$$\frac{d}{dt}n(t) = S(t) + \frac{(\rho - \beta)}{\Lambda} n(t) + \sum_i \lambda_i C_i(t) \quad (7a)$$

$$\frac{d}{dt}C_i(t) = \frac{\beta_i}{\Lambda} n(t) - \lambda_i C_i(t) \quad (7b)$$

Where $n(t)$ is the total number of neutrons at time t , $C_i(t)$ is number of radioactive precursors of group i and half-life of $t_{i/2}$, $S(t)$ is the number of neutrons introduced at time t by the start-up source, ρ is the reactivity, k is the multiplication factor, β is the total sum of the delayed neutron fraction for each of the six groups β_i , Λ is the prompt generation time, and λ_i is the decay constant of each i -th group.

This theory demonstrates the general behavior of a multiplying system through equations that model neutron population. The understanding of this equation during reactor operation analytically demonstrated what the reactor behavior would be if there was no prompt neutrons being produced from fission, and that the decay heat being generated was due solely from the delayed neutrons produced from radioactive decay. Understanding this theory allowed for the understanding the basis of decay heat in a real core, the core simulation, isotope production and decay within the core, and to better approach and develop methods for validation of results produced from the simulation.

The reason the results and code for the simulation needed validation was to make sure that the data was viable and accurately reflected a real phenomenon in a nuclear reactor core. One of the approaches used to validate that the code was accurately showing real core behavior was by examining the decay heat being generated by and the population of two fission products isotopes. The isotopes chosen were Iodine-135 and Xenon-135. The reason these isotopes were chosen was because of their particular behavior after the reactor has been shut down. As shown in the production schemes below, Xenon-135 is actually a

radioactive daughter of Iodine-135 while both are actually fission products of Uranium-235. Xenon-135 usually reaches its equilibrium balance of production and decay at approximately 50 hours after the reactor has been operating at a constant power. At this equilibrium balance the population of Xenon-135 remains at a constant value. This balance represents that Xenon-135 is being produced at the same rate (from fission and decay of Iodine-135) that it is decaying.^[6]

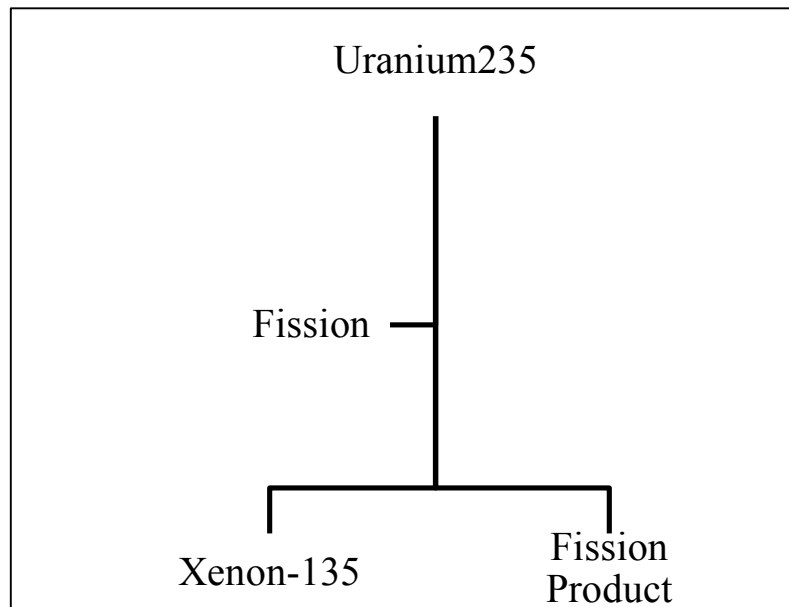


FIG.1. Xenon-135 production scheme

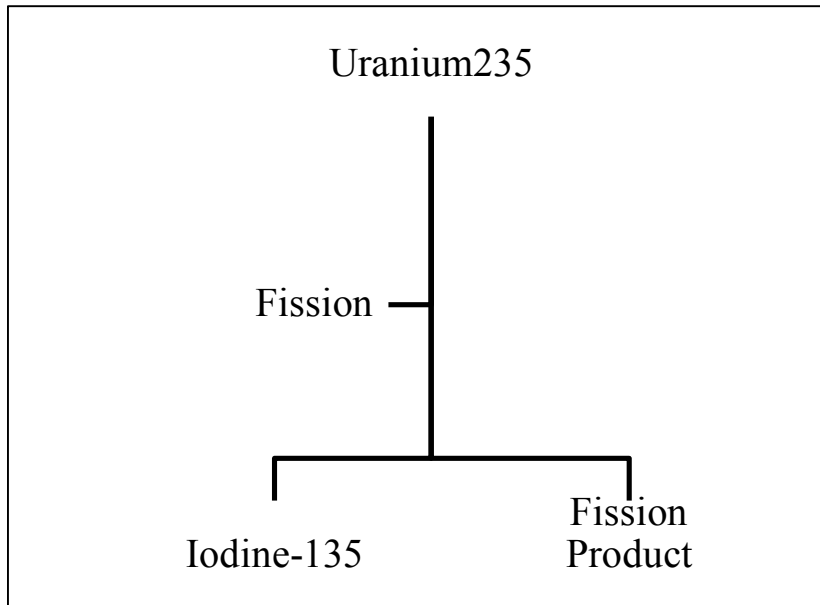


FIG.2. Iodine-135 production scheme

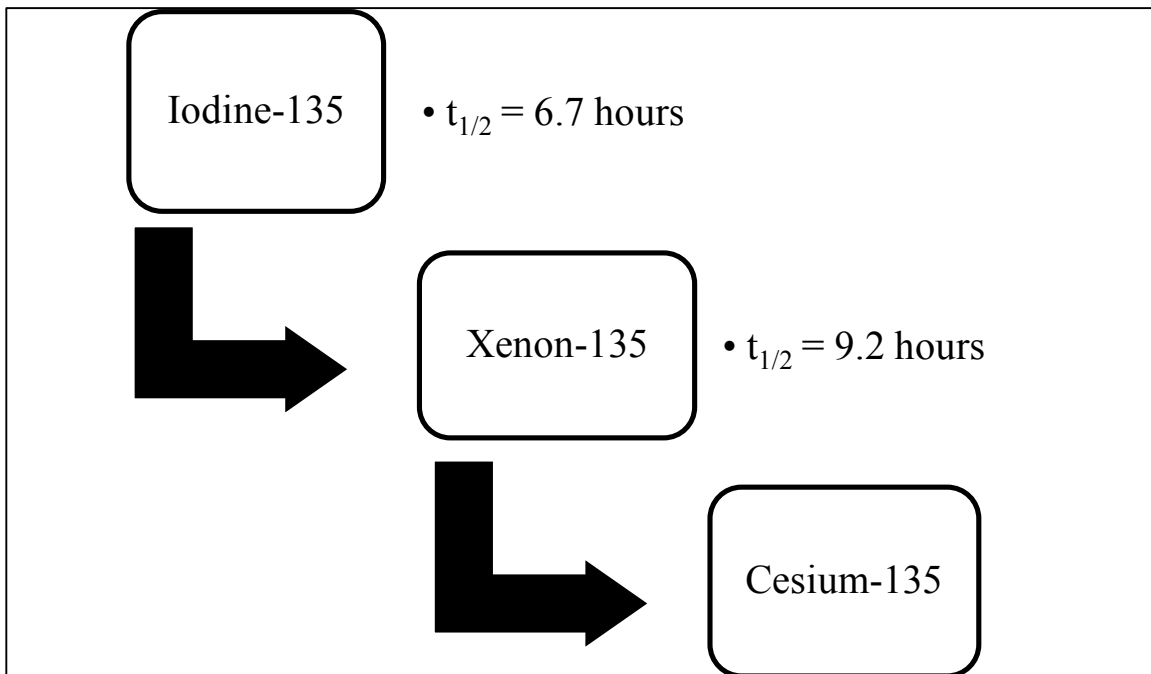


FIG.3. Xenon-135 and Iodine-135 decay scheme

These schemes showed that the half-life of Iodine-135 is actually noticeably shorter than that of Xenon-135. This led to conclusion that in a real core, and thus in the simulation used for the project, after the reactor scram event happens and decay heat starts to be

produced, Iodine-135 and Xenon population should start to decrease as they decay away. It is to be noted that there should be a noticeable build-up of Xenon-135 for the first few minutes or hours immediately following the scram as Iodine-135 is decaying into Xenon-135 faster than what it is decaying into Caesium-135. After several hours though, the population of Iodine-135 would be so low that it would no longer cause a build-up, so therefore the Xenon-135 population would start to decrease as well. This method allowed verified that our decay heat curve was accurate by measuring the population of these isotopes in the core after the scram, and the decay heat they generated.

The second method used to validate the simulation code involved numerical calculations from an equation provided by Dr. Warren D. Reece of Texas A&M Nuclear Engineering Nuclear Science Center and his laboratory exercise titled “Reactor Pool Calorimetrics”.^[7] The equation for a numerical approximation of decay heat in a nuclear reactor is shown below.

$$P_{decay} = 0.066P_0[(t_s)^{-0.2} - (t_s + \tau_s)^{-0.2}] \quad (8)$$

Where P_{decay} is the decay heat generated as a function of time, P_o is the full power at which the reactor previously operated, t_s is the time since the reactor was shut down, and τ_s is the previous operating time.

This equation allowed for a numerical approximation of the decay heat for any value after the shutdown event for up to 100 days after shutdown. This approximation does not produce any isotopic data of the core though, and is only an approximation based on time and full power of the reactor, leading to the conclusion that it would only serve as a guideline to the data produced by the simulation. The reason being that the simulation

takes into account the specific layout of the core, fuel composition, burnup of the fuel, fuel enrichment, and fuel mass of the core.

III.A.2 Background Research

The input deck that generated the data used for this project needed to be based on actual design specifications of an existing BWR with an RCIC system. This BWR needed to be similar to Unit 1 at the Fukushima Daiichi plant so as to better correlate the data to the event. The site and its corresponding data chosen as a basis for the neutronics analysis was the Monticello Nuclear Generating Plant due to the accessibility of the technical specifications of the core. The general plant specifications of both sites are shown below.^{[2][3]}

Table 1. General specifications for both sites

	Monticello Nuclear Generating Station	Fukushima Daiichi Unit 1
Reactor Power [MWe]	610	460
Reactor Power [MWth]	1469	1380
Reactor Type	GE BWR-3	GE BWR-4
Fuel Assembly Layout	7x7	7x7
Containment	Mark I	Mark I

This comparison showed that the reactor chosen as a basis for the model was of a comparable size and output, and provided good data for the input deck of the simulation.

While the typical burnup of the fuel for both units was unknown, it was found that typically it varies between 20-40 GWd/MTU. The methodology section below provides more input parameters used to model the Monticello Nuclear Generating Station core in the simulation software.

III.A.3 Methodology

The different methodologies shown below thoroughly describe the processes and methods used to generate the simulation and data, along with the data that was used for validation using the numerical approximation. These methods were chosen for this project based on observations that concluded analytically from the theory and equations shown and described in the Theory and Relevant Equations subsection above. The following methods used the thermal value of the reactor power provided above over the electrical power output, since it is the thermal output what is being determined in the decay heat analysis.

III.A.3.1 Hand Calculations for Decay Heat Approximation

Before undertaking the decay heat simulation with the modeling software, a basis needed to be established as a tool for comparison and validation to ensure that the model and the data produced adhered to the reactor kinetics theory already established. This was achieved by calculating Eq. (8) at increasing values of time after the scram, t_s , with a step of 10 seconds between calculations up to the first 1.2 hours, and with a step of 30 minutes for the remainder of the calculations up to a total time of 72 hours. These values were then plotted on Microsoft Excel to give a visual representation of what the decay heat generation curve should look like. The basic parameters used for the equation are shown in the table below.

Table 2. Input parameters for decay heat approximation equation.

Power During Reactor Operation [P _o]	Time Reactor Was Operational [τ _s]	Range	Total Number of Steps
1469 MW	365 Days	0 – 72 Hours	479

The reason for the large amount of data calculated was to provide a consistent and reliable comparison for the decay heat curve generated by the model. For the sake of thoroughness, this data was later calculated again using the time steps used in the simulation for ease of comparison, once the initial comparison with the large data set had been made.

III.A.3.2 ORIGEN-ARP Decay Heat Simulation

ORIGEN-ARP was the software selected to model the decay heat of the reactor core used for this analysis. ORIGEN-ARP is a module of the SCALE6.1 suite developed at Oak Ridge National Laboratory. It is actually a sequence that provides fast results from the calculations of the ORIGEN-S code using the Automatic Rapid Processing (ARP) algorithm that allows for the generation of cross-section libraries from the interpolation of pre-generated libraries. These interpolations are performed on burnup, enrichment, and water density.^[8] The input for the ORIGEN-ARP deck required several parameters that were found in the Final Safety Analysis Report (FSAR) of the Monticello Nuclear Generating Station, under the reactor core section. As stated previously in the Background research, the actual burnup of the fuel is unknown, so for this simulation two decks were created. One deck was coded to produce the results of a burnup of 20 GWd/MTU while the other deck was coded to produce the results of a burnup of 30 GWd/MTU. These values were chosen since the background research found them to be typical values of burnup in a

BWR. The rest of the parameter values required to construct the ORIGEN-ARP input deck are shown below and were drawn from the FSAR of the Monticello Nuclear Generating Station. ^[3]

Table 3. ORIGEN-ARP input parameters for Monticello Nuclear Generating Station Unit

Parameter	Value [Unit]
Reactor Power	1469 [MW]
Time Operating at Full Power	365 [days]
Decay Time	72 [hours]
Decay Time Steps	13
Fuel Enrichment	2.03 [wt% U-235]
Fuel Assembly Layout	GE 7x7
Number of Assemblies	484
Mass of Fuel/Assembly	223.48 [kg]
Total Mass of Fuel in the Core	108,164.32 [kg]
Type of Fuel	UO ₂

All of these input parameters were constant for both input decks, and each one was set up to have two separate outputs at different 13 different time steps as described above. The values of each step are shown in the table below.

Table 4. ORIGEN-ARP time step values

Step #	Value [hours]
1	1.00E-03
2	3.00E-03
3	1.00E-02
4	3.00E-02
5	1.00E-01
6	3.00E-01
7	5.00E-01
8	1.50E+00
9	4.50E+00
10	1.35E+01
11	2.40E+01
12	3.00E+01
13	7.20E+01

This distribution of time steps allowed for a most of the points of data to be generated early on the decay heat curve with respect to time. The reason this was done was because it is at this time that decay heat is changing the most for all isotopes since the short-lived radioactive isotopes are decaying quickly. Once the equation stabilized and most of the decay heat was being generated by the longer lived isotopes, then bigger time steps were taken.

The ORIGEN-ARP input deck was set up to create two output decks as mentioned above, each deck providing different data about the isotopes created during operation and during the decay heat generation stage after the shutdown. The first output consisted of the decay heat generated by each individual isotope in watts at different time values. From this output file the total decay heat at different values was just a summation of the individual isotope

decay heats. The decay heat data for the isotopes Iodine-135 and Xenon-135 was also taken from this output file. The second file was only designed to give the concentration in grams per unit volume [cm^3] of the core of these same two isotopes. This data from both output files was then used to ensure that the core behaved as predicted analytically by reactor kinetic theory and model shown above during operation and after the scram event. This validation ensured that the total decay heat data made sense and was a viable result. Once all of the data was obtained, it was plotted by the Microsoft Excel software and analyzed.

III.B. THERMAL HYDRAULICS

With the decay heat calculation from the neutronics calculations the modeling of the fluid flow in the reactor and RCIC system was performed using RELAP5. The code applies the conservation of mass, momentum, and energy equations to the system to analyze the thermal-hydraulic characteristics of the system. Creating an input deck for the code required the determination of the parameters of the subsystems, such as the pump and turbine specifications. Since a majority of the information regarding the specifications of plant components is proprietary, a best estimate had to be used in the RELAP5 input deck. With the best estimate for the parameters and specifications, the next step was to write an input deck.

The main components of the input deck, as seen in the nodalization of the coolant system in Fig. 4, are the reactor, condensate storage tank, suppression pool, turbine, and pump.

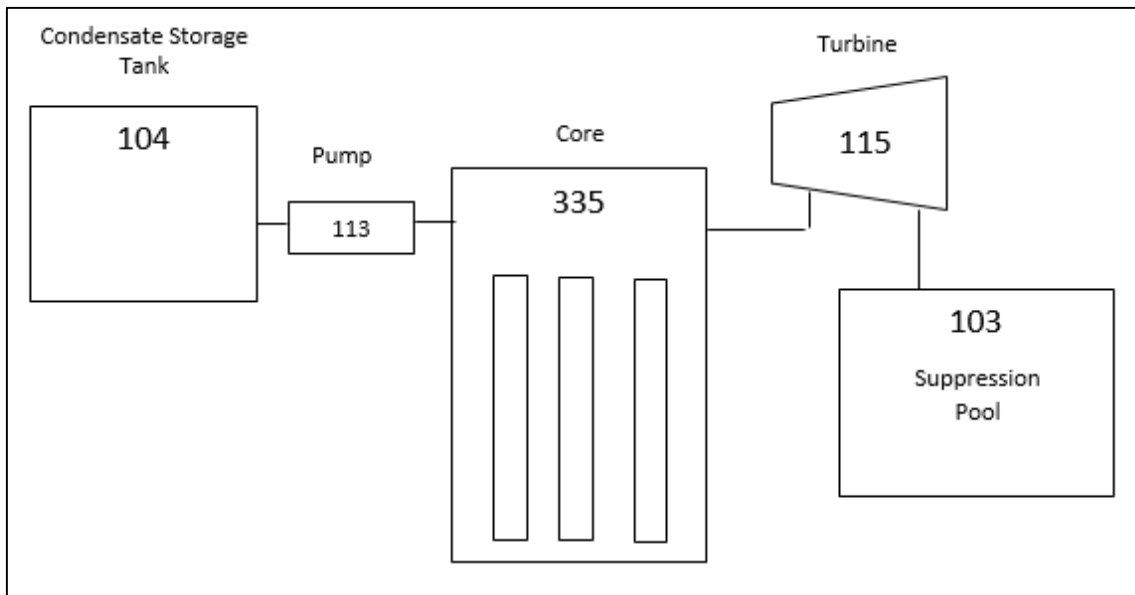


FIG.4. Nodalization of the existing RCIC system

The condensate storage tank and suppression pool were the simplest aspect of the input deck. They were each modeled as a single volume. The reactor pressure vessel was much more complicated. For this reason a simple RELAP5 input deck of a PWR was modified and used in the RCIC input deck. Although there are many significant differences between a PWR and BWR, the pressure vessel of the PWR could replace the pressure vessel of the BWR in our calculations because the flow through the vessel itself is of little concern to this project. The most challenging components to model were the pump and turbine.

The turbine and pump were difficult to model since, as stated previously, the specifications of the components are proprietary. The turbine and pump in RELAP5 is modeled as a specialized branch. The turbine was modeled with a single stage and the pump was modeled to have a maximum capacity of 700 gpm and no reverse rotation. The RCIC system is designed such that the turbine and pump are connected along a common shaft. This, however, was not done in the input deck due to the complexity of the coding

requirements that it would introduce. It was assumed that since research indicated the amount of flow that the RCIC system can provide is known, as long as the pump did not exceed this value, the results of the analysis would be realistic. The code allowed for the evaluation of how the system functions as a whole. Once the current system was analyzed, modifications to the system and the RELAP5 input deck were made in an attempt to lengthen the amount of time that the RCIC system can cool the reactor.

There are multiple reasons why the RCIC system is expected to shut down within 12 hours of operation, however, with time constraints considered, it was only feasible to focus on just one of the reasons it ceases to function. With some research, it was determined that the focus would be placed on the heat of the room where the turbine and pump are located. Since the flow of steam through the turbine generates a significant amount of heat, it is expected that the room will eventually become too hot for the system to operate. Thus, the modification that was made to the system was the addition of a heat exchanger and fan in the room and thereby extending the amount of time the system can operate.

Once the calculations for the amount of fluid that needed to flow through the heat exchanger and drive the fan were completed the heat removal components were modeled in RELAP5. Figure 5 shows how the heat exchanger was placed in the RCIC loop.

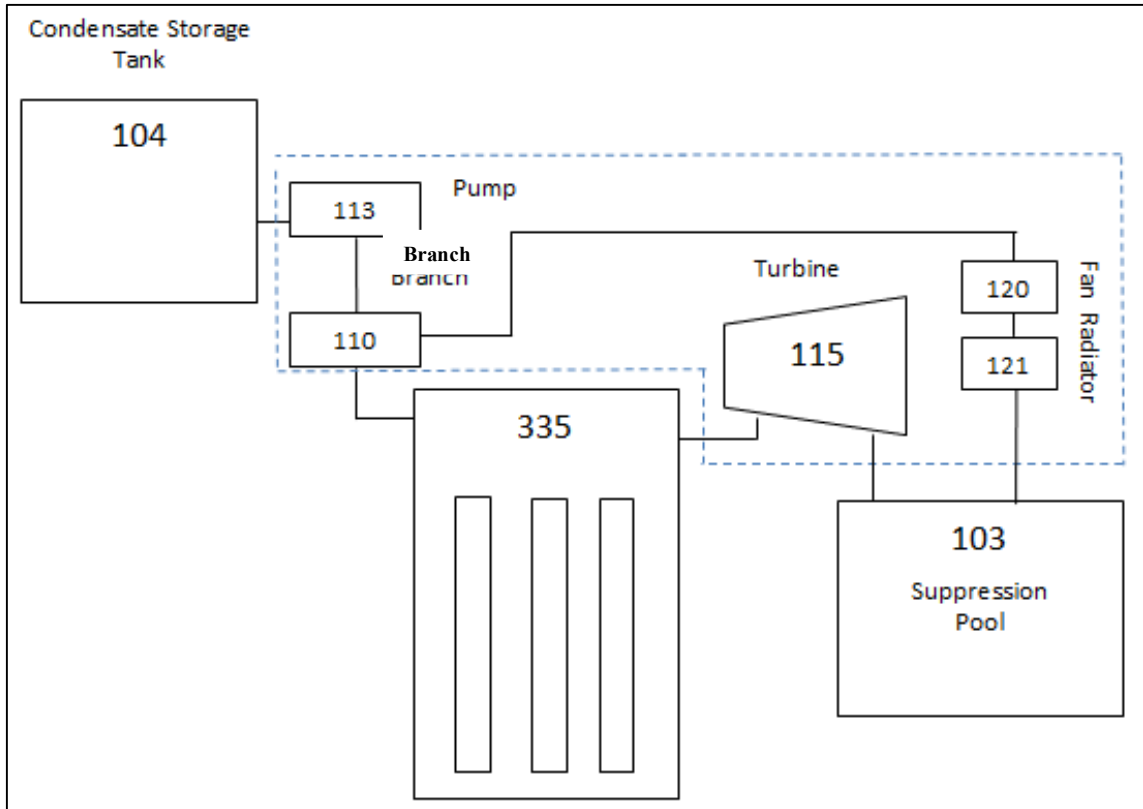


FIG.5. Nodalization of the modifications made to the RCIC system.

The nodalization shows how the modifications were modeled. It was done by having a branch that would divert the required flow at the right pressure from the RCIC pump to the suppression pool to simulate the presence of a heat exchanger.

Another parameter that was considered was the amount of coolant available to the system. The RCIC system has two locations at which it can draw suction. It can draw a suction from the condensate storage tank and the suppression pool. Using the coolant in the suppression pool is challenging since it also happens to be the location where the steam from the turbine is exhausted. The steam is exhausted through a sparger below the surface of the coolant. Therefore, the location of the sparger and suction are key to the problem. If the intake for the RCIC is relatively close to the sparger the heat of the coolant could be

much higher than expected. It could even mean that some steam bubbles could be sucked into the system. Since the location of the sparger and the location where the RCIC system draws its suction are unknown, it was decided that the modeling of the system would only involve cooling the core with the coolant inventory located in the condensate storage tank. It was determined, through research, that the condensate storage tank will normally contain enough coolant to cool the core for approximately 19 hours.^[4]

III.C. SYSTEM MODIFICATIONS

The first step in designing a heat sink for any system is calculating the heat that it is required to be removed from the system. Modeling the heat transfer exactly from an intricate turbine model without dimensions is an incredibly difficult task. Because of this, some assumptions were necessary to get the numbers that were needed. For the turbine, a rectangular geometry, a surface temperature of 287.2 Celsius, and that any radiation the turbine emits was negligible and had no effect on the overall heat transfer was assumed. It was also assumed that the temperature of the room that contained the turbine had an air temperature of 20 Celsius. The film temperature of the surface was then calculated using Eq. (9) below.^[9]

$$T_f = \frac{T_s + T_\infty}{2} = \frac{287.2 + 20}{2} = 153.6 \text{ }^\circ\text{C} \quad (9)$$

The properties of air at the approximate temperature were looked up, using linear interpolation to obtain the properties at the film temperature. These properties were used to determine the approximate heat loss from the surface of the turbine. These estimates for the temperatures will lead to a conservative estimate of the heat loss from the turbine, meaning the estimate will be greater than the actual heat loss. They are conservative

because the actual surface temperature of the turbine will not actually be 287.2 Celsius. This is because that is about the temperature of the steam that is flowing from the core through the turbine. Once inside the turbine, there are many other heat transfer processes that occur before the heat even propagates all the way to the surface of the turbine. The conservativeness of the heat loss calculation will allow the design of a heat sink that will have the capacity to remove heat from the air faster than the turbine can put heat into the air with almost certainty.

To calculate the total heat loss from the turbine, it is necessary to calculate the heat loss from each side of the model, then sum the results. The surface heat loss by free convection from the vertical sides and horizontal top and bottom is given by Eq. (10).^[9]

$$q = 2q_s + q_t + q_b + q_f$$

$$q = (2\bar{h}_s * A_{s,s} + \bar{h}_t * A_{s,t} + \bar{h}_b * A_{s,b} + \bar{h}_f A_{s,f})(T_s - T_\infty) \quad (10)$$

To calculate the convection coefficients corresponding to each of the sides, the Rayleigh number must be known. The Rayleigh number was calculated using Eq. (11) below.^[9]

$$Ra_L = \frac{g\beta(T_s + T_\infty)L^3}{\nu\alpha} \quad (11)$$

The Rayleigh number was needed to determine the flow of the free convection boundary layer. Once the flow regime was known, the Nusselt number was determined utilizing the appropriate equation. These equations are listed below for their respective applications in Eqs. (12) – (14).^[9]

$$\text{Upper surface:} \quad \overline{Nu}_L = .15Ra_L^{1/3} \quad (10^7 \leq Ra_L \leq 10^{11}, \quad \text{all } Pr) \quad (12)$$

$$\text{Lower surface:} \quad \overline{Nu}_L = .52Ra_L^{1/5} \quad (10^4 \leq Ra_L \leq 10^9, \quad Pr \geq .7) \quad (13)$$

$$\text{All other surfaces: } \overline{Nu}_L = 0.68 + \frac{0.670Ra_L^{1/3}}{\left[1 + \left(\frac{.492}{Pr}\right)^{9/16}\right]^{4/9}} \quad (Ra_L \leq 10^9) \quad (14)$$

Using the Nusselt number, the convection coefficients for each of the sides were attainable using the equation below.^[9]

$$\bar{h} = \frac{k}{L} \overline{Nu}_L \quad (15)$$

All of the determined convection coefficients were then plugged into Eq. (15) and the total heat loss was found. This value then became the required heat transfer from the air in the design of the heat sink. Due to power restrictions due to the station blackout, a shell and tube heat exchanger with the cold fluid being pumped through the tubes via the RCIC pump was determined to be the most favorable design. Also, this water flow circulation would power the fan that would push the air through the heat exchanger at a given flow rate. The task then became to calculate the general specifications of the heat exchanger that would be able to remove the necessary amount of heat from the air. Some specifications that were needed to be found were as follows: number of tubes, length of tubes, length and diameter of the shell, and inlet and outlet temperatures. The type of heat exchanger that was chosen for the design was the shell and tube heat exchanger. Some of the reasons this type of heat exchanger was because this design is less expensive relative to other heat exchanger designs and easier to maintain than other designs.^[10] Figure 6 depicts an approximate desired design of the shell and tube heat exchanger for this system.

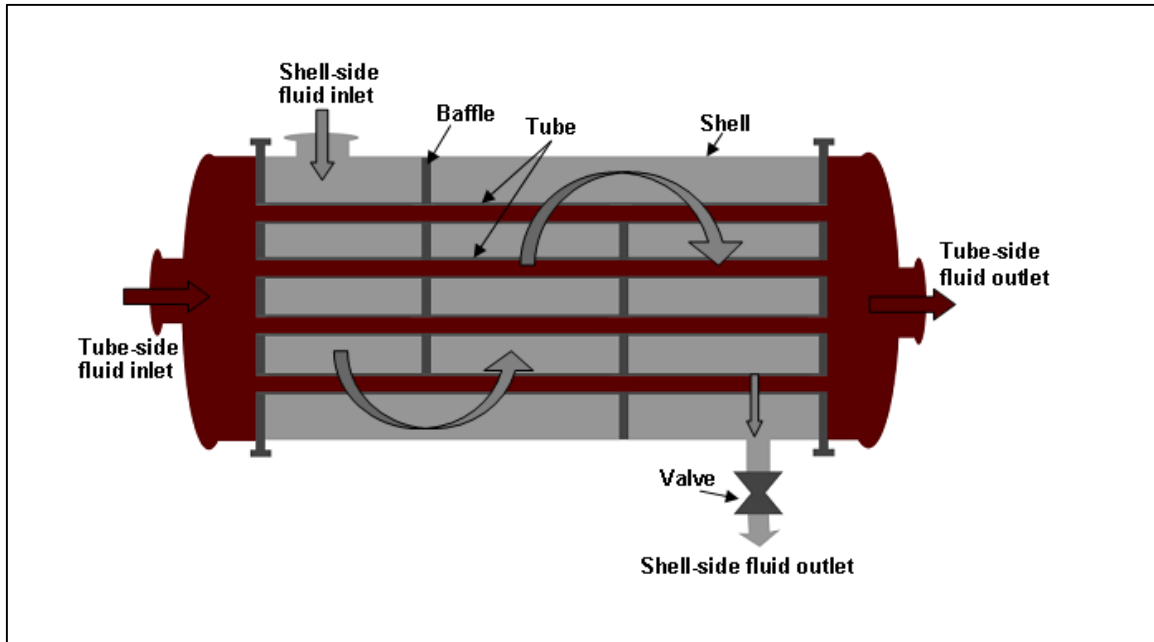


FIG.6. Design of a shell and tube heat exchanger.

For this design, the total heat transfer rate from the turbine to the surrounding air was used as the required heat exchange from the hot side to the cold side in the heat exchanger. This is also a conservative estimation because in reality the heat exchanger will not be directly next to the turbine. The distance separating the two components leads to a temperature gradient throughout the air itself, decreasing the amount of heat available to transfer to the cold side of the heat exchanger. One of the goals is to make this heat exchanger as easy to incorporate into the current operational RCIC system, this includes the overall cost of the integration. Therefore, one of the design requirements is to minimize the size of the heat exchanger because that leads to a reduced total cost and an easier and faster installation. In the design adherence as closely as possible to the calculated heat transfer rate as to not incur additional costs was imperative.

To calculate the specifications of the heat exchanger, the following equations were used in the hand calculations.^[9]

$$\bar{h}_{h,o} = \bar{h}_{h,i} - \frac{q}{\dot{m}_h c_{p,h}} \quad (16)$$

$$\bar{h}_{c,o} = \bar{h}_{c,i} + \frac{q}{\dot{m}_c c_{p,c}} \quad (17)$$

$$Re_D = \frac{4\dot{m}_c}{\pi D \mu} \quad (18)$$

$$Nu_D = \frac{\left(\frac{f}{8}\right) (Re_D - 1000) Pr}{1 + 12.7 \left(\frac{f}{8}\right)^{1/2} (Pr^{2/3} - 1)} \quad (19)$$

$$f = (.79 \ln(Re_D) - 1.64)^{-2} \quad (20)$$

Once the Nusselt number is known, Eq. (15) is then used to find the heat transfer coefficient of the heat exchanger. These hand solutions were then plugged into the Kamlex Heat Exchanger software to determine the required characteristics of the heat exchanger.^[11]

IV. DISCUSSION

IV.A. NEUTRONICS

Once the input decks for ORGIEN-ARP were created, and the hand calculations for decay heat approximation were set up using the parameters and approach described above, the output data was collected and exported to Microsoft Excel. In this spreadsheet software, the data was plotted and validated. The results of the simulation along with a discussion of their meaning and implications is shown below.

IV.A.1 Hand Calculations for Decay Heat Approximation

As described previously, this method was meant to provide a numerical basis and an approximation of what a decay heat curve looks like. Using the approach outlined in the theory section above with the parameters defined in the methodology section, the following results were produced outlining the decay heat generation in Watts as a function of time in hours.

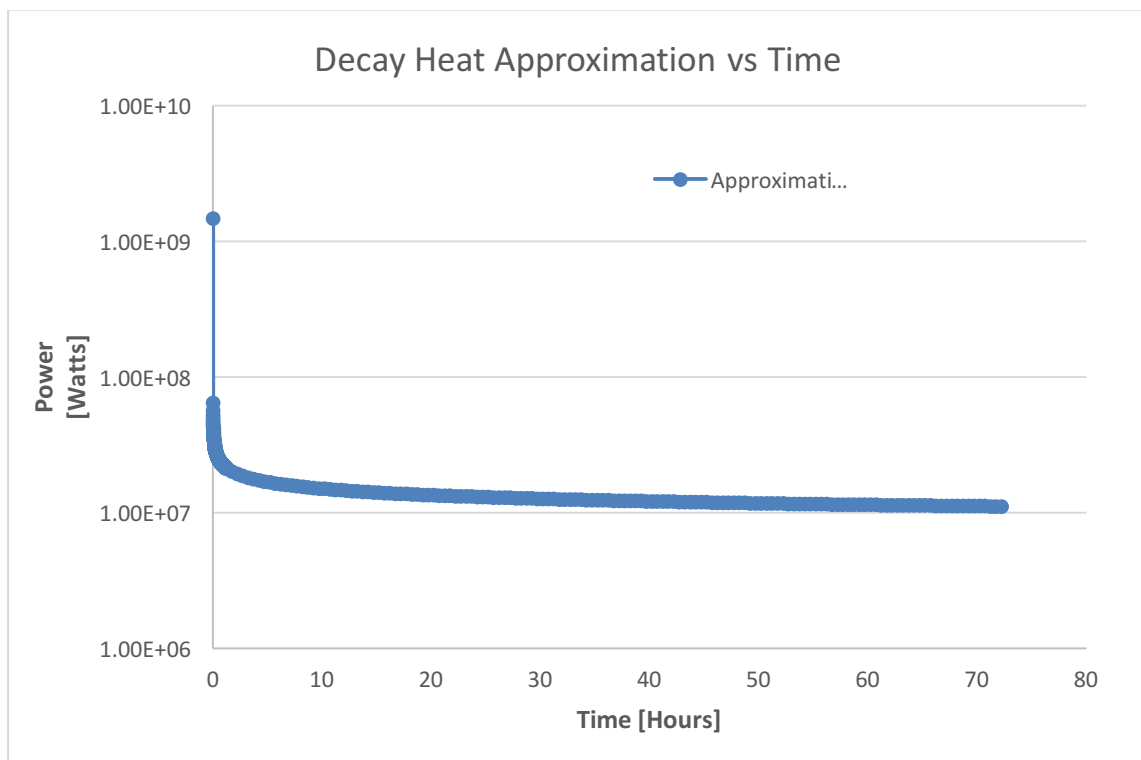


FIG.7. Numerical hand decay heat approximation vs time

Several observations and conclusions were made from Fig. 7. It was assumed that at time $t = 0$ the reactor was at full power, and that it was at this time that the scram event happened. It was observed that at the 10 second mark after the scram, the decay heat of the reactor was already more than one degree of magnitude smaller. This presents the loss of heat generation from fission caused by all prompt neutrons leaving only the production of

delayed neutrons from the 6 groups as discussed in the theory section and demonstrated in Eqs. (7a) and (7b). It was also noted that for the first minutes after the reactor scram, the amount of heat produced at each step rapidly decreased as time increased. Given what was understood from reactor kinetics theory and the relationship of delayed neutron precursor decay constants to the delayed neutron population, this rapidly decreasing trend was assumed to be caused by the short-lived isotopes decaying away. At approximately 10 hours after the scram, it was observed that the curve had stabilized and had a relatively small slope that continued to decrease for the remainder of the time. It was concluded that this point the short-lived delayed neutron precursors and isotopes were no longer contributing a significant amount of neutrons to the population and that the decay heat was now being generated by the long lived isotopes and delayed neutron precursors.

These observations were in accordance with the theory established and provided a numerical approximation method to increase the understanding of the behavior of the core and of the decay heat curve that were generated from the ORIGEN-ARP data.

IV.A.2 ORIGEN-ARP Decay Heat Simulation

After the numerical approximation for decay heat was calculated, the ORIGEN-ARP decks were ran under the SCALE6.1 suite graphical user interface (GUI) using the parameters and methodology described previously. Overall 4 output files were created and 8 different plots were produced from the 2 input decks generated for the different burnups.

IV.A.2.1 Results for 20 GWd/MTU Burnup

The first deck provided results for a core simulation in which the burnup of the fuel was equivalent to 20 GWd/MTU, with all other parameters equivalent to those previously

defined in the background research and methodology, which are consistent with the core specifications of the Monticello Nuclear Generating Plant. The first plot to be produced and analyzed from the output file was a plot of the decay heat contributed by the 10 isotopes with the highest initial decay heat out of the 40 generated by ORIGEN-ARP, over the entire time frame.

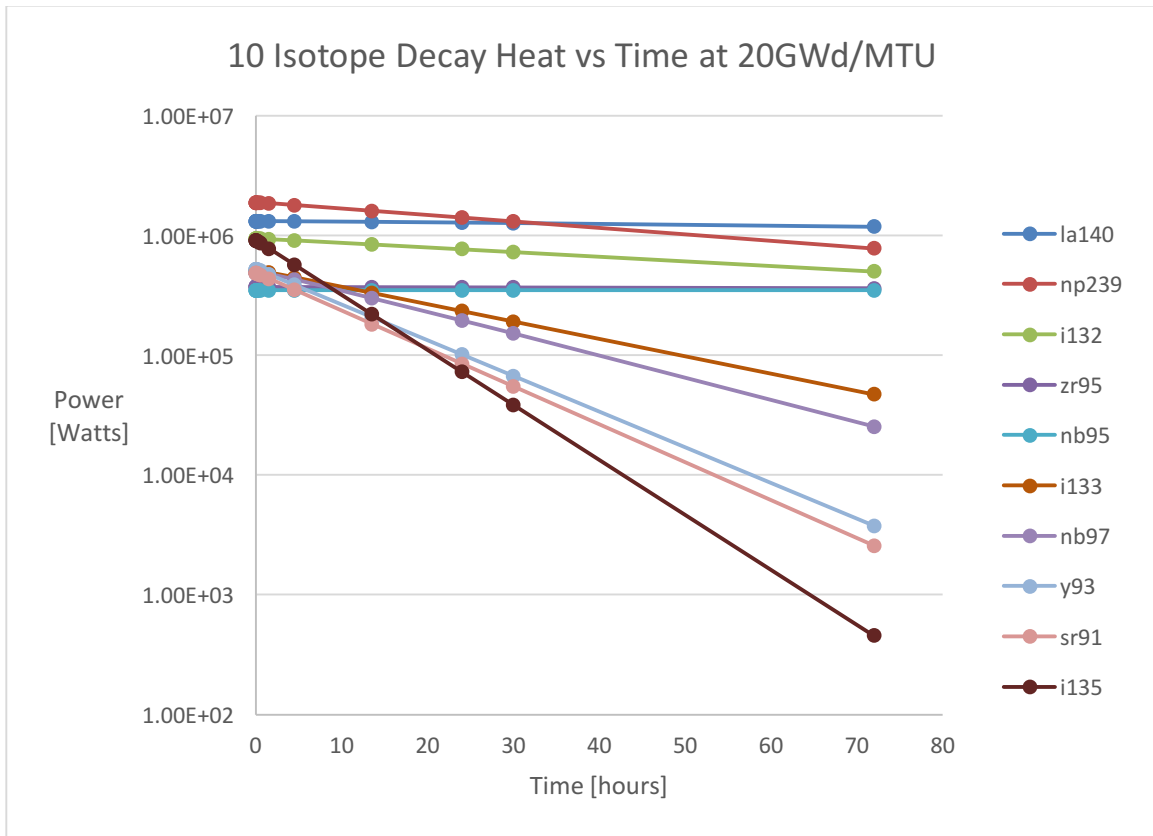


FIG.8. Top Ten isotopes with the highest initial decay heat contribution as a function of time for a 20GWd/MTU burnup.

These ten decay heat generating isotopes in the core and the decay heat they contributed as a function of time, were deemed relevant in that they showed showed that several isotopes do in fact have a significantly shorter half-life than others. Some of these short lived isotopes, which have the most negative slope on this graph, were also noticed to contribute

a large amount of decay heat early on in the curve, and after the 10 hour mark, they seem to no longer be large contributors to the total decay heat. It is of particular note that the power was plotted on a logarithmic scale for this graph, meaning that these isotopes produced large amounts of heat for a short period of time before losing orders of magnitude in the amount of heat generated. These observations were deemed to be in accordance with the analytical conclusions arrived at in the theory section above, and seemed to correspond to the total decay heat curve that was calculated numerically. Once this was established, then the total decay heat from the total number of isotopes was plotted with respect to time.

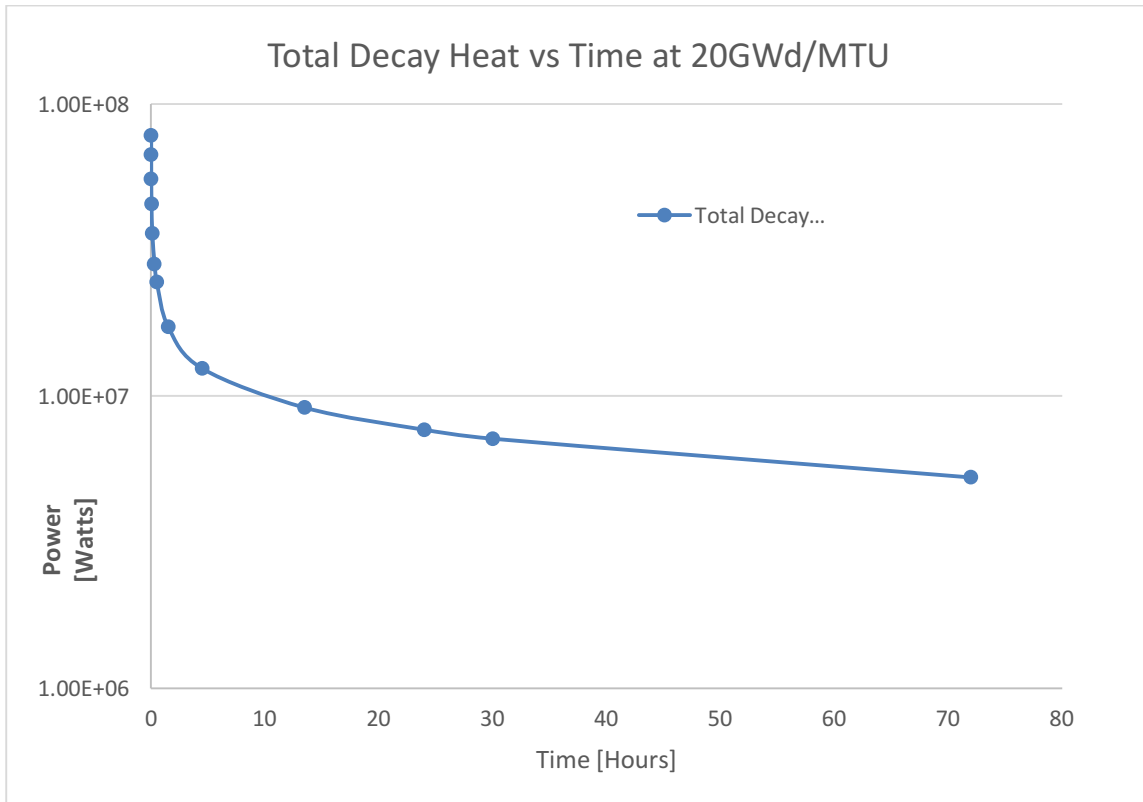


FIG.9. Total decay heat from all isotopes as a function of time for a 20GWd/MTU burnup.

Figure 9 shows the plot and corresponding curve of the decay heat analysis generated by ORIGEN-ARP. Each point is a summation of the decay heat generated by all of the isotopes

produced by ORIGEN-ARP and found in Appendix A. The first observation made from this graph was that the curve function does seem to match that of the numerical approximation and the conclusions reached at in the theory section. This led to the conclusion that the output was in fact behaving as expected in an analytical comparison with Fig. 7. The data produced was then analyzed using the analytical method described in the theory section where the decay heat generation from Iodine-135 and Xenon-135 and their corresponding populations would be plotted to see if they followed the expected buildup of Xenon-135 deduced from the decay schemes shown in Figs. 1-3.

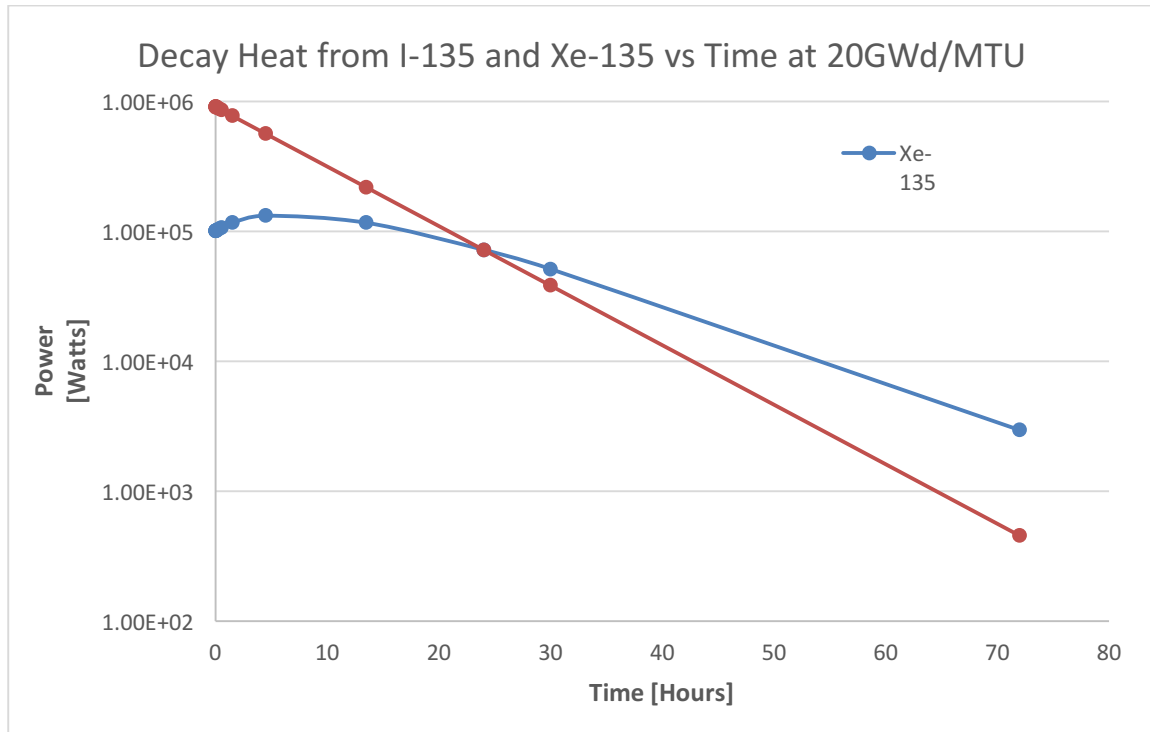


FIG.10. Decay heat generation from Iodine-135 and Xenon-135 as a function of time at 20GWd/MTU burnup.

The decay heat curves produced by Iodine-135 and Xenon-135 shown in Fig. 10, coincide with the conclusions drawn from both the theory and decay scheme of these isotopes. As time increases the decay heat generated by Iodine-135 quickly decreases by several orders

of magnitude. However, Xenon-135 actually sees an increase in the decay heat it generates for the first 10 hours or so, so that it's higher than the equilibrium that was established during operation and at $t = 0$ for the decay heat analysis. As explained earlier, this is due to Xenon-135 having a longer half-life than Iodine-135 and thus creating a bottleneck and an accumulation of Xenon-135. Only after Iodine-135 goes below a certain threshold, where the decay of Xenon-135 is larger than the production of it from radioactive decay, is the decay heat generated by the decaying Xenon-135 observed to begin to decrease. These observations were based on the correlation that the amount of decay heat generated from decay is directly proportional to the population of the isotopes. To further ensure that this statement is valid, the density of these isotopes in mass per unit volume of fuel [g/cm^3] were plotted during the decay heat time and analyzed.

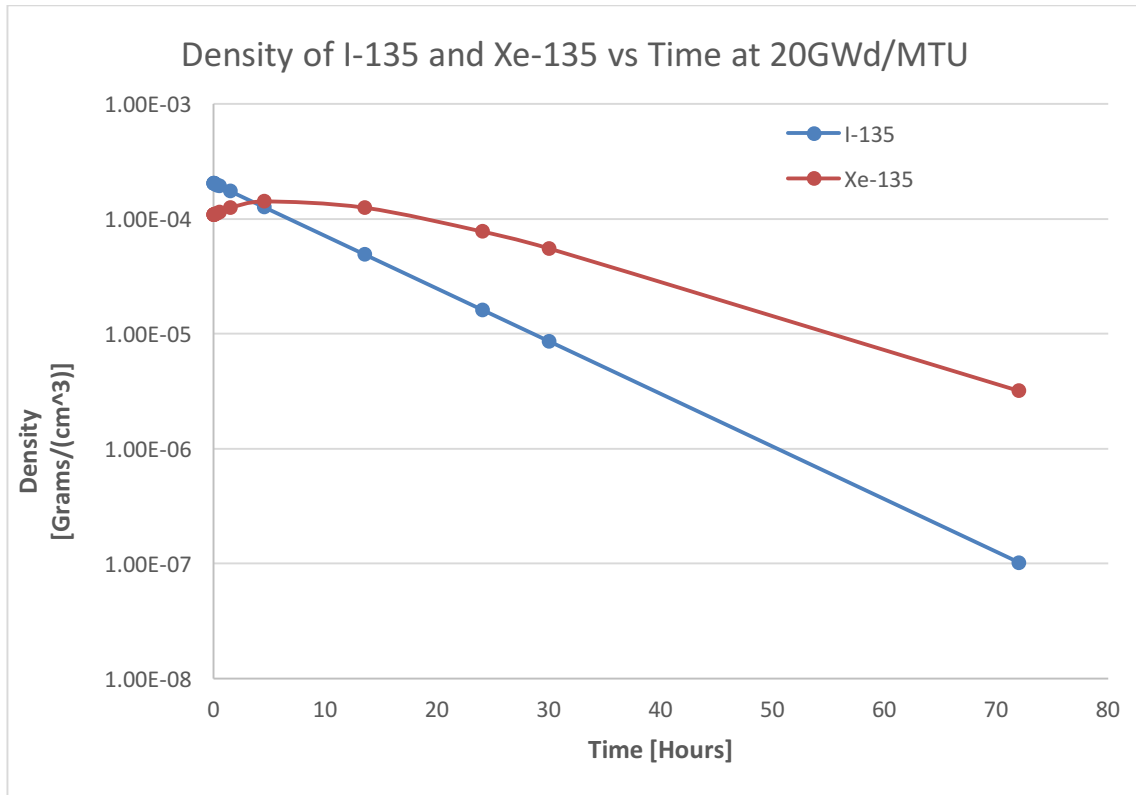


FIG.11. Density of Iodine-135 and Xenon-135 in fuel as a function of time for 20GWd/MTU burnup.

The results plotted for the actual density of these isotopes in the fuel seem to be in accordance with both the theory established, and with the decay heat for these isotopes shown in Fig. 10. From an analytical perspective, the outputs generated by the ORIGEN-ARP input deck for 20GWd/MTU burnup were found to be in accordance with the theories presented earlier.

IV.A.2.2 Results for 30 GWd/MTU Burnup

Like the first deck, the second deck provided results for a core simulation, but for this deck the burnup of the fuel was changed to 30 GWd/MTU. All other parameters were equivalent to those previously defined in the background research and methodology and the first deck,

which are consistent with the core specifications of the Monticello Nuclear Generating Plant. Again, the first plot to be produced and analyzed from the output file was a plot of the decay heat contributed by the ten isotopes with the highest initial decay heat with respect to time.

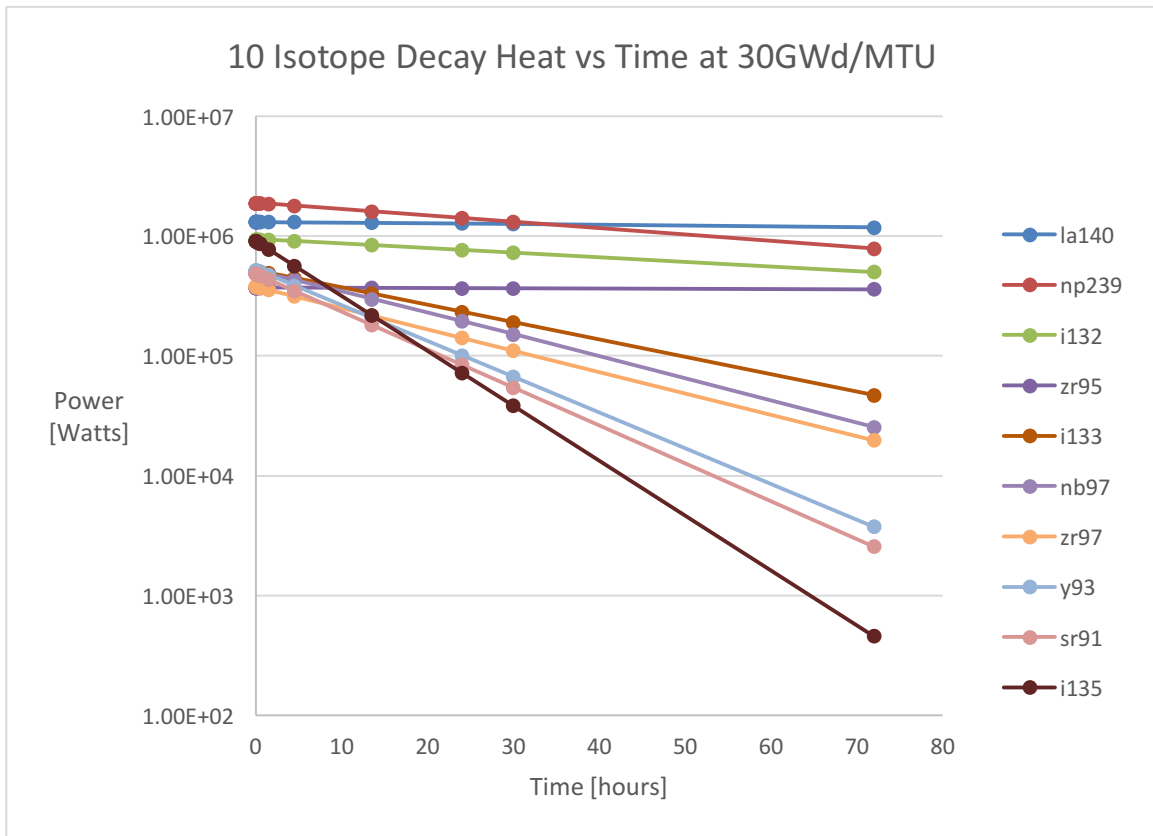


FIG.12. Top Ten isotopes with the highest initial decay heat contribution as a function of time for a 30GWd/MTU burnup.

Figure 12, shown above, contains the 10 decay heat generating isotopes with the highest initial decay heat generation in the core as a function of time just like Fig. 8. This data plot again showed that some short lived isotopes, which have the most negative slope on this graph, contribute a large amount of decay heat early on in the curve, and after the 10 hour mark, they seem to no longer be large contributors to the total decay heat. These

observations were deemed to be in accordance with the analytical conclusions arrived at in the theory section above, the conclusions reached from the analysis of the output of the deck at 20GWd/MTU burnup, and seemed to correspond to the total decay heat curve that was calculated numerically. After all these verifications, the total decay heat from these isotopes was plotted with respect to time.

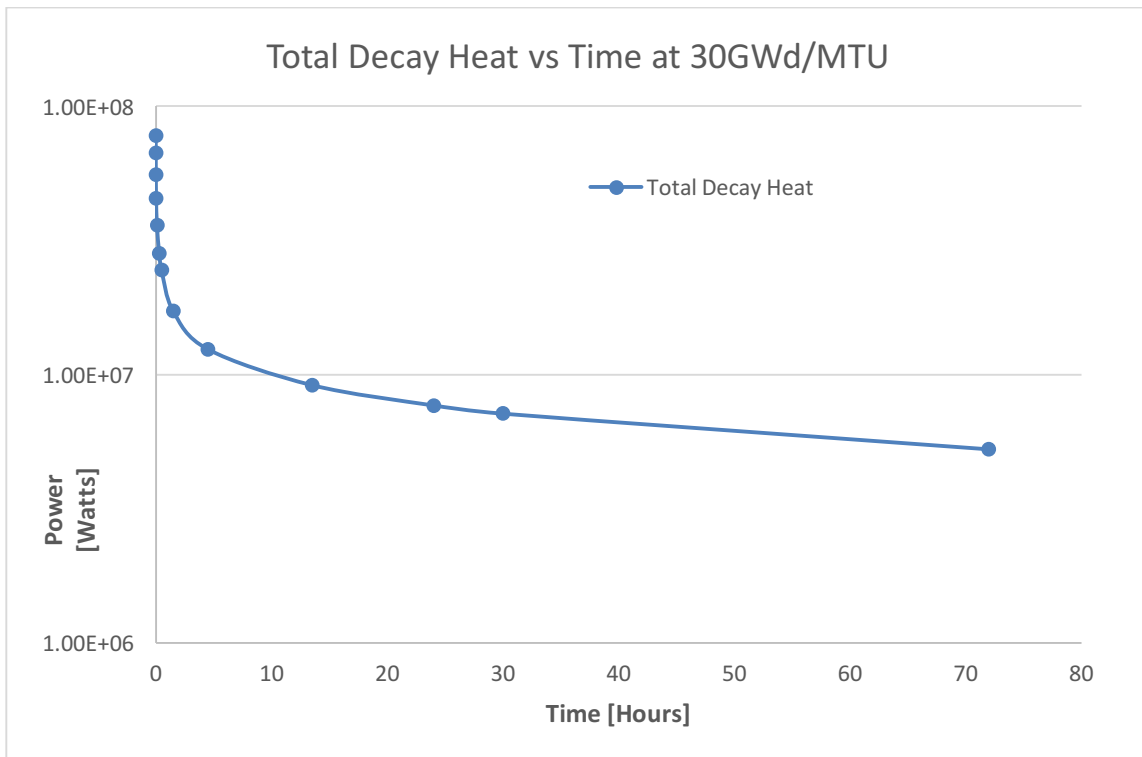


FIG.13. Total decay heat from all isotopes as a function of time for a 20GWd/MTU burnup

Each data point in Fig. 13 above is a summation of the decay heat generated by all of the isotopes shown in Fig. 12. These points and curve again seem to match the values obtained from the numerical approximation and the conclusions reached in the theory section. It was again concluded that the output was in agreement with the output at 20GWd/MTU burnup, and the curve function seemed to be of the same shape as that of Fig. 4. The data was then

analyzed again by examining the decay heat and populations of Iodine-135 and Xenon-135 as with the first output file.

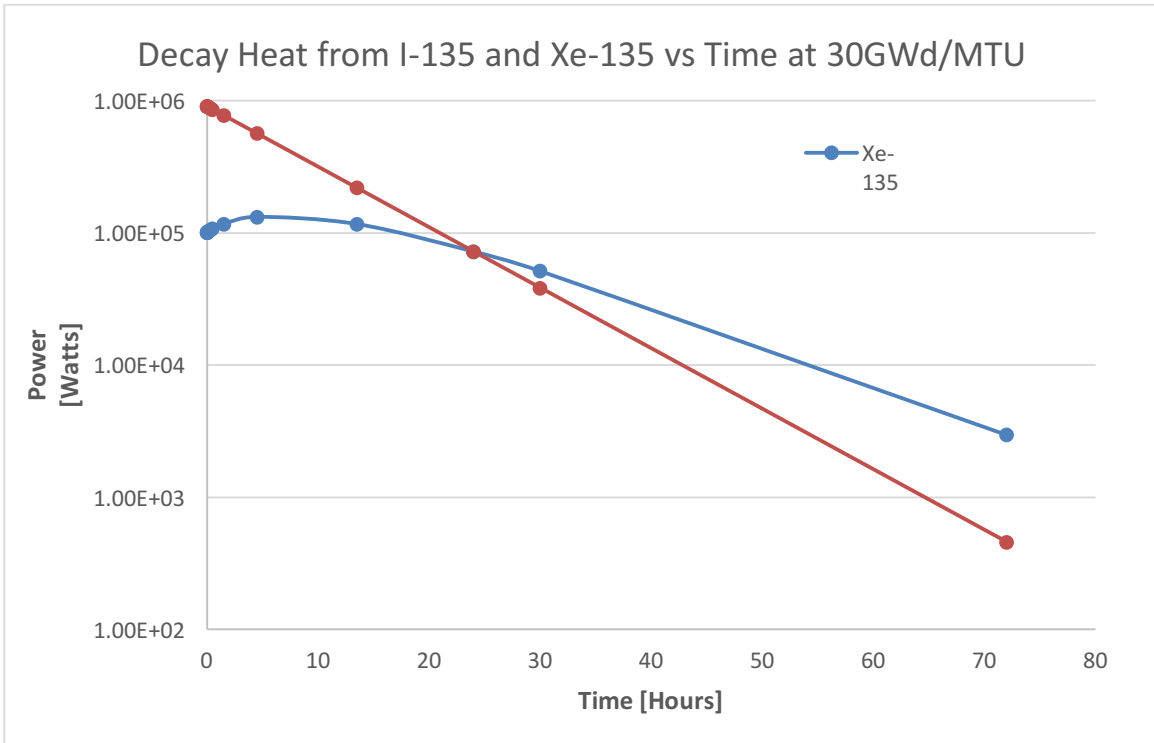


FIG.14. Decay heat generation from Iodine-135 and Xenon-135 as a function of time at 30GWd/MTU burnup.

The decay heat curves were found to again be in agreement with the phenomena described in the theory and in the previous output result and analysis. The increase of decay heat generated from Xenon-135 was again accredited to the buildup of Xenon-135 from the bottleneck caused by the quick decay of Iodine-135. Again to ensure that there was a correlation between the populations of these isotopes to the decay heat generated by them, their density for the volume of the fuel as a function of time was also plotted.

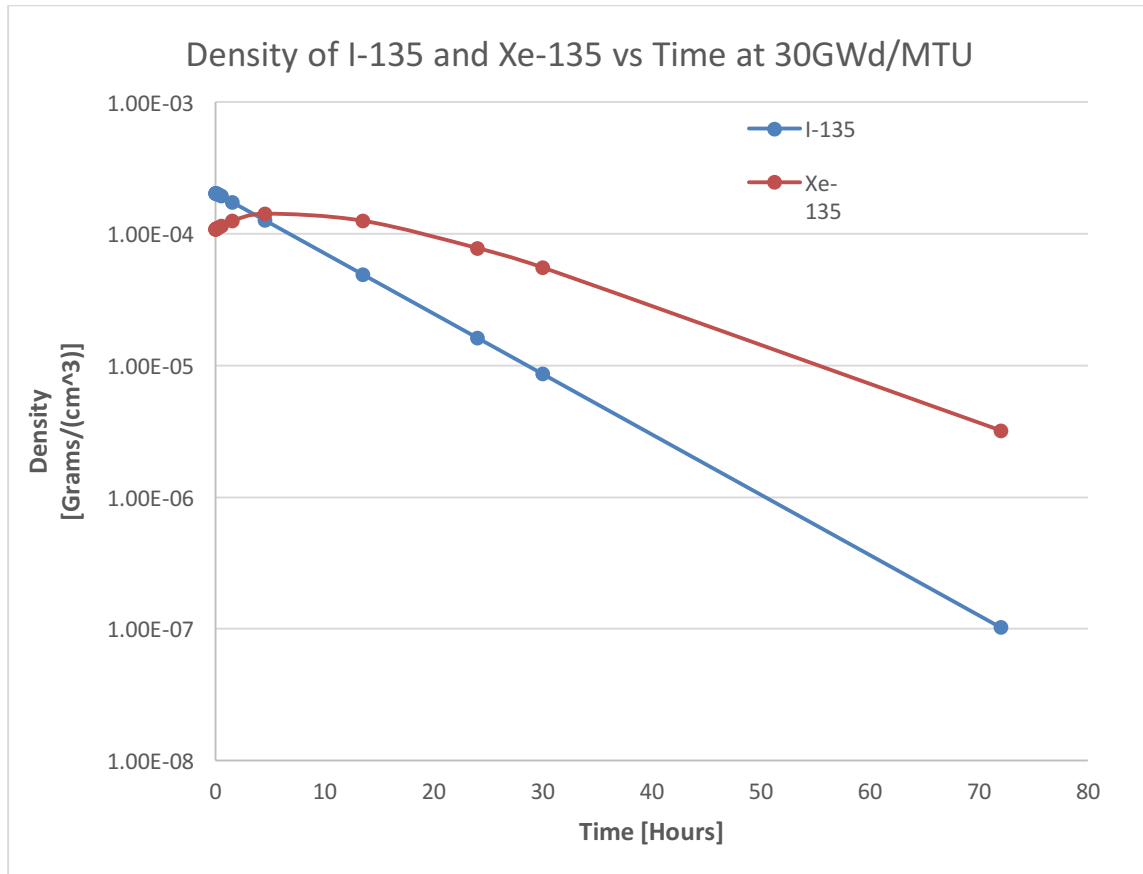


FIG.15. Density of Iodine-135 and Xenon-135 in fuel as a function of time for 20GWd/MTU burnup.

This plot was again in agreement with the results found in the previous input deck and with the theory previously established. As the population of Iodine-135 decreased rapidly, it caused a buildup of Xenon-135 due to its longer half-life. These outputs were found to be in accordance with all analytical validation methods and approaches and were deemed to be viable results for the project.

IV.A.3 ORIGEN-ARP Results vs Decay Heat Estimates

After the results were plotted and compared to the theory and each other in an analytical fashion, they were then compared to each other numerically. In order to do so, the results

from ORIGEN-ARP and the decay heat estimates arrived at numerically, were plotted on the same graph and with the same time steps. The best way to do this was to use the time steps defined in Table 4, with Eq. (8). This produced results at the same time values as the simulation for ease of comparison.

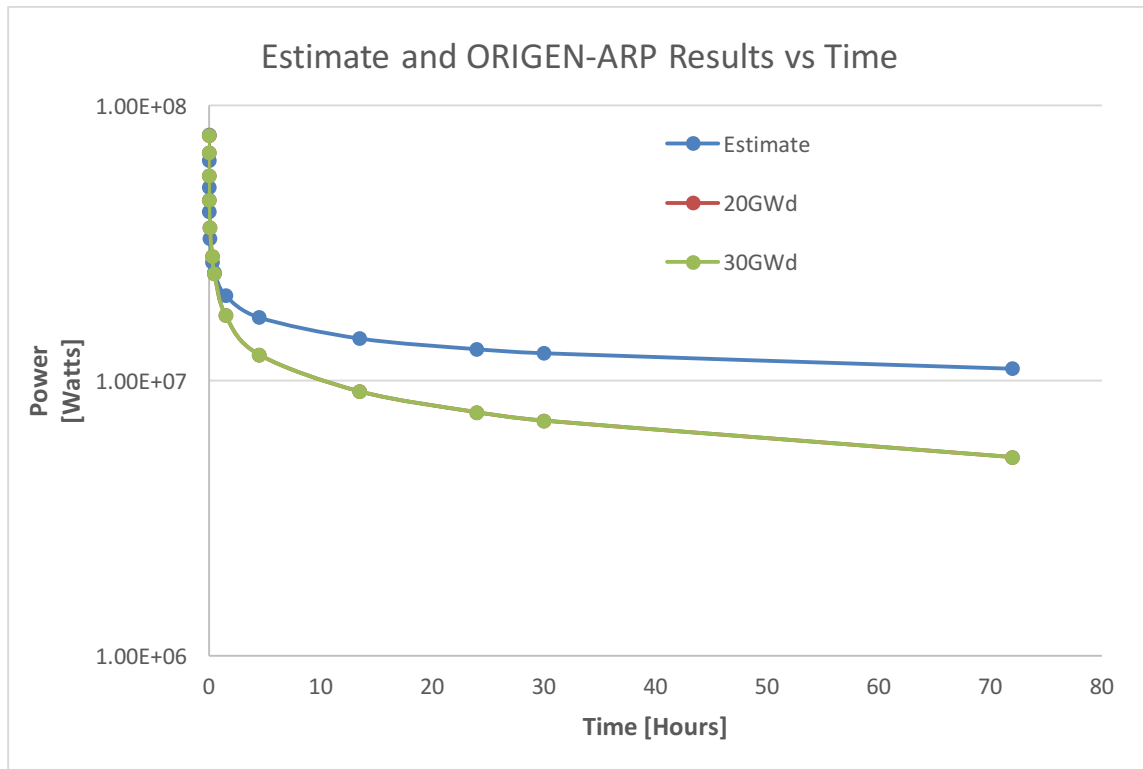


FIG.16. Estimated and ORIGEN-ARP Results as a function of time.

Figure 16 provides a basis for comparing both decay heats from ORIGEN-ARP and the estimate generated from Eq. (8). This plot shows that the difference between the two burnups was actually not that great on the total decay heat curve, and that the differences between the approximation and the simulation results are actually not that large, varying less than an order magnitude at its largest gap. For the sake of thoroughness, these values were also put in a chart as seen below.

Table 5. ORIGEN-ARP results and approximation numerical comparison.

Time [Hours]	Decay Heat at 20GWd/ MTU burnup [W]	Decay Heat at 30GWd/ MTU burnup [W]	Approx. [W]	Percent Difference (20GWd/MTU burnup)	Percent Difference (20GWd/MTU burnup)
1.00E-03	7.79E+07	7.79E+07	7.81E+07	0.23	0.22
3.00E-03	6.72E+07	6.73E+07	6.33E+07	-6.21	-6.23
1.00E-02	5.55E+07	5.56E+07	5.04E+07	-10.16	-10.18
3.00E-02	4.54E+07	4.54E+07	4.11E+07	-10.58	-10.60
1.00E-01	3.61E+07	3.61E+07	3.29E+07	-9.55	-9.59
3.00E-01	2.83E+07	2.83E+07	2.70E+07	-4.66	-4.70
5.00E-01	2.45E+07	2.45E+07	2.47E+07	0.77	0.73
1.50E+00	1.73E+07	1.73E+07	2.04E+07	15.60	15.55
4.50E+00	1.24E+07	1.24E+07	1.70E+07	26.97	26.91
1.35E+01	9.14E+06	9.15E+06	1.43E+07	35.96	35.91
2.40E+01	7.68E+06	7.69E+06	1.31E+07	41.16	41.11
3.00E+01	7.16E+06	7.16E+06	1.26E+07	43.27	43.23
7.20E+01	5.27E+06	5.28E+06	1.11E+07	52.42	52.39

Both Table 5 and Fig. 16 show that for up to 0.5 hours after the reactor is scrammed, the absolute value of the difference between the simulation and the approximation is less than 10%. Only towards the end of the time period are larger deviations observed. The reason for this was actually determined to lie in the theory behind the numerical approximation. The fact that this approximation did not take into account core design data such as fuel composition, enrichment, layout, and can be used for any reactor BWR, PWR, TRIGA, etc., led to the conclusion that this approximation would not lie exactly on the curve

generated by the model. However due to the close values produced by ORIGEN-ARP and the values of the approximation, and the similar curve trend seen in both the results and the approximation, the results were deemed realistic and acceptable for use on the project.

IV.B. THERMAL HYDRAULICS

The first step in the modeling of the RCIC system was to write an input deck for RELAP5 that would accurately predict the thermal characteristics of the system. Since the exact specifications of the system were largely unknown, a best estimate was used. The main characteristics that were used to validate the input deck were the flow rate of the pump and the heat generated by the core.

The amount of flow that the RCIC system can be expected to produce is within a range from 300 to 800 gpm.^[12] The results from the RELAP5 input deck was a mass flow rate of around 37 kg/s which is approximately 586 gpm, as seen in Fig. 17.

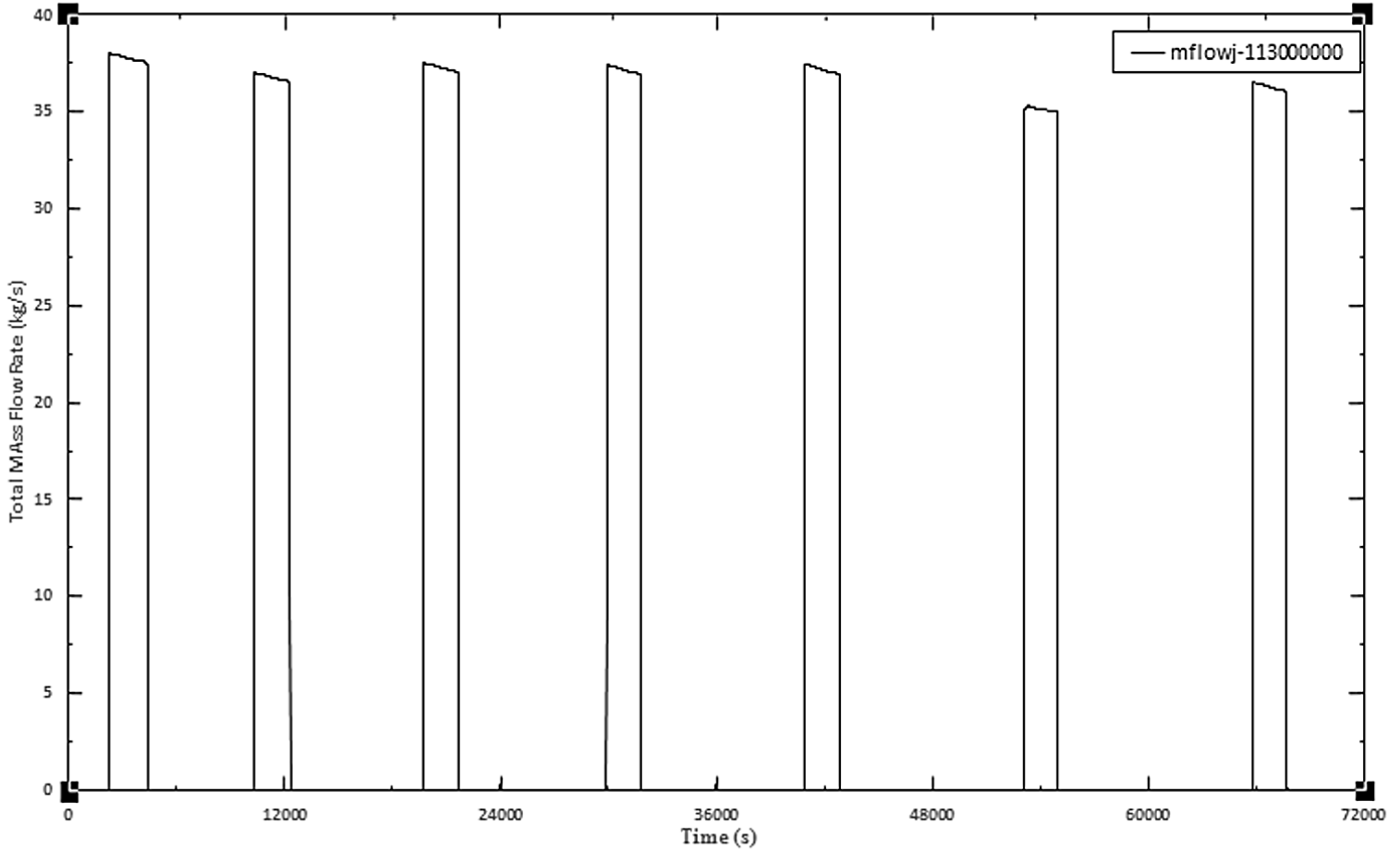


FIG.17. Total mass flow rate through the RCIC pump.

Since the mass flow rate of the model is well within the given limits it is an indication that the model, at least the pump, is functioning correctly. In the figure, it is also seen that the amount of time that the RCIC system remains shutoff begins to increase the longer that the reactor has been shutdown. This is the result of the decay heat decreasing over time. The decrease in heat means that the amount of coolant lost to boiling is also decreased. Another parameter that is important to observe is the volume of coolant in the condensate storage tank. The condensate storage void fraction was recorded in Fig. 18.

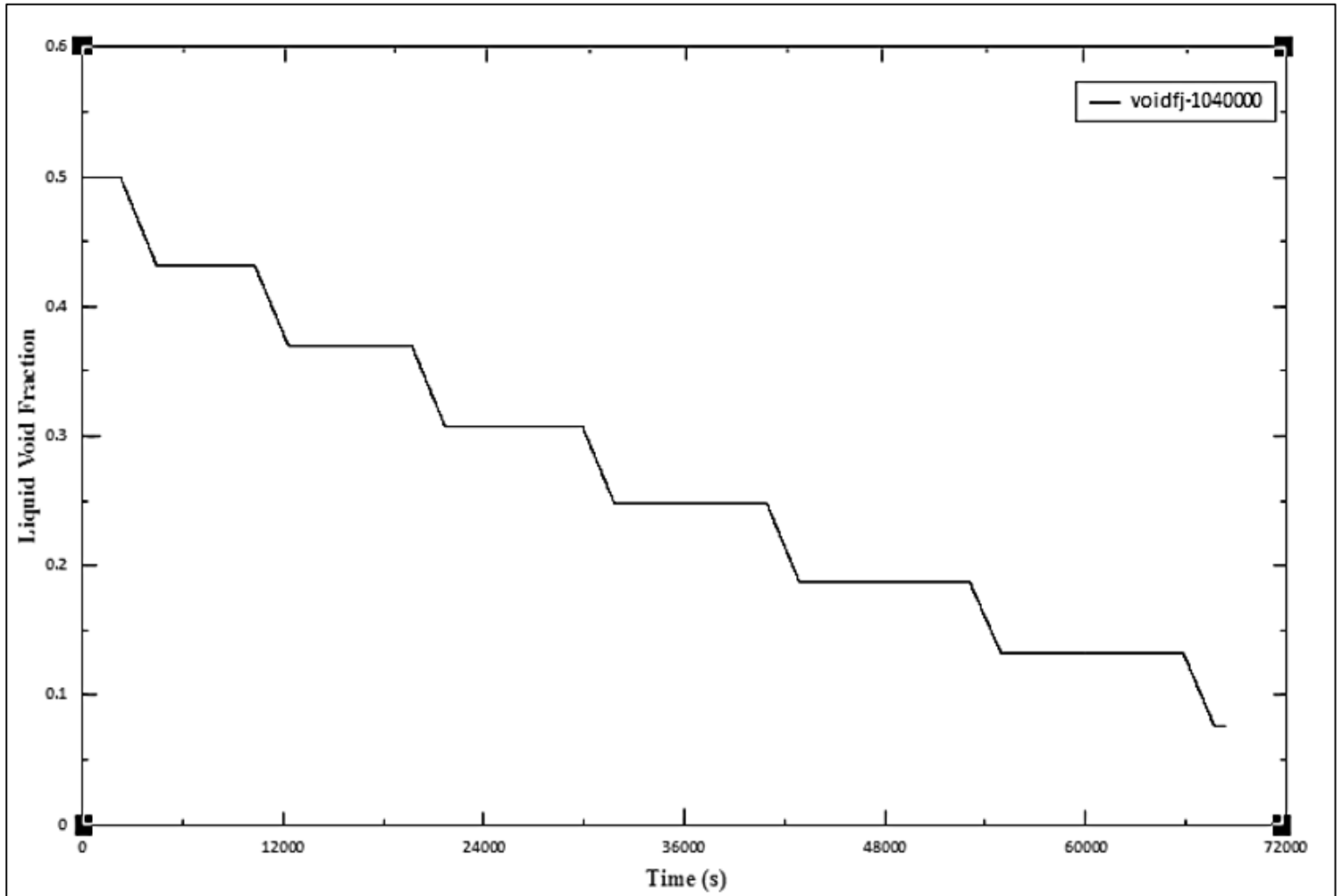


FIG.18. Plot of the volume of the condensate storage tank

The liquid void fraction is defined as the amount of liquid in the tank divided by the total volume of the tank. This value is important since once the condensate storage tank is empty the RCIC pump must take a suction from the suppression pool, which is out of the scope of this project. The way that the input deck was written once the reactor core void fraction falls below 82.5% the RCIC system is turned on and once it reaches a value of 97% it is turned off. Although the actual values for when the system is turned on and off is not known, a value was chosen that would ensure that the core never became uncovered. Thus, in Fig. 19 the oscillations of the void fraction for the core can be seen.

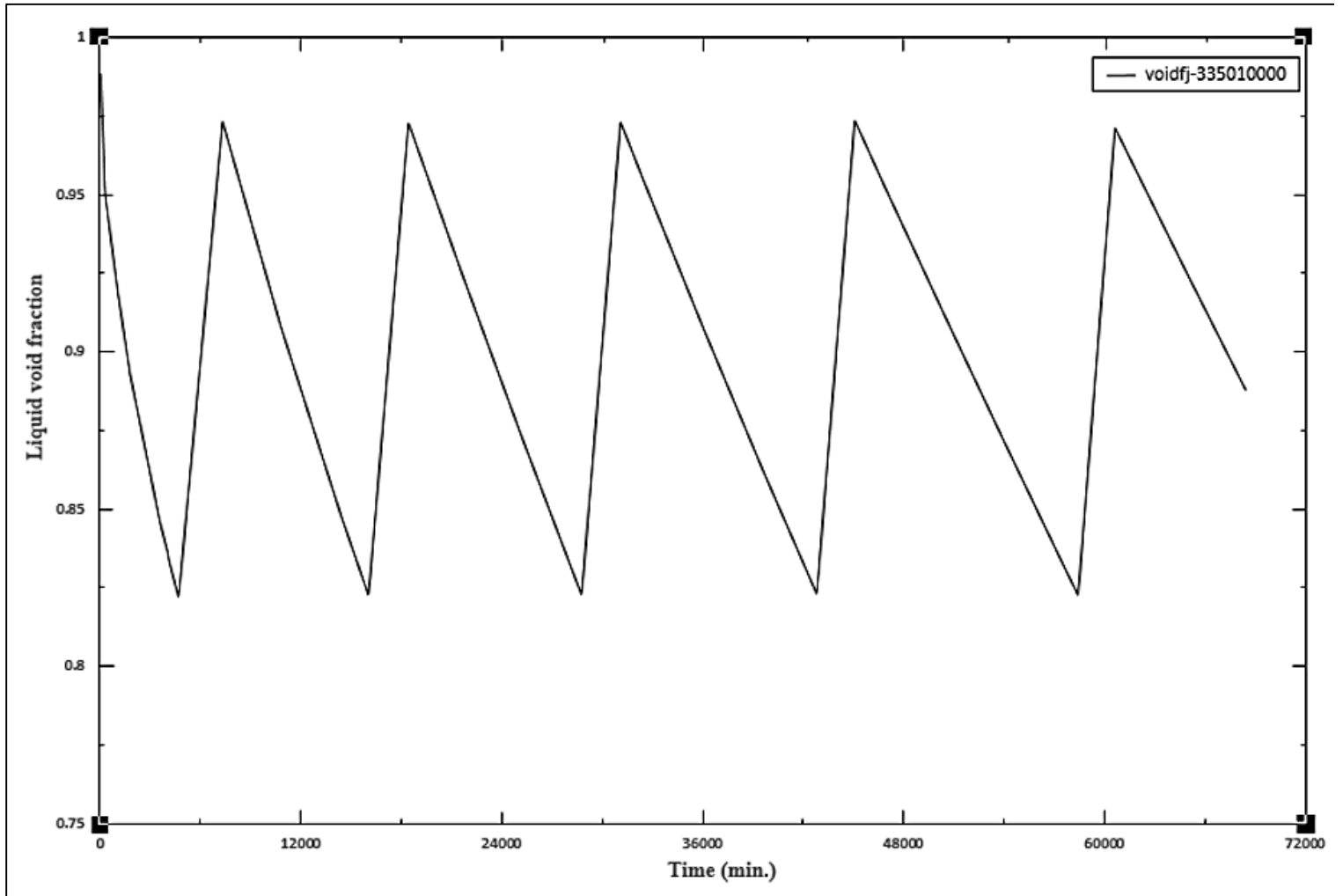


FIG.19. Void fraction that correlates the amount of coolant in the core.

It was found from these graphs, given that the system does not fail, the RCIC system will be capable to operate for 19 hours with only the condensate storage tank for coolant. The next process was to model the system with some of the flow being diverted to the heat exchanger. The system had to be remodeled to ensure that the condensate storage tank will still have enough coolant inventory. Also, it was important to validate that the RCIC pump was adequate to produce enough flow to keep the core full while also providing coolant to the heat exchanger and fan cooling system.

With the results from the hand calculations of how much coolant is needed to cool the room, the heat exchanger was modeled using a branch that diverted some of the flow directly to the suppression pool instead of through the reactor pressure vessel.

IV.C. SYSTEM MODIFICATIONS

Table 6 depicts all of the values that were assumed for the turbine.

Table 6. Table of assumed values for the heat transfer away from the turbine.

	Assumed Value
Length	2 m
Width	1 m
Height	1.5 m
T_s	287.2 °C
T_∞	20 °C

Table 7 illustrates the assumed values for variables that were used in the analysis of the heat exchanger. Each assumption was made based on a conservative estimate of the system.

Table 7. Assumed values used in the calculations for the heat exchanger design.

	Assumed Value
$T_{h,o}$	30 °C
$T_{c,i}$	20 °C
\dot{m}_h	.910492 kg/s
\dot{m}_c	7.78 kg/s

The values for the mass flow rate were determined by the fan that was selected for use in the system as the source of air flow. The selected fan is a CSZ – 380. The fan’s specifications are listed below in Table 8.

Table 8. Specifications for the Chun Hao Axial Flow CSZ-380 Explosion Proof Exhaust Fan^[13]

\dot{m}_{air}	4000 – 10000 m^3/hr
\dot{m}_{water}	28 – 53 m^3/hr
P_{water}	.2 – .5 MPa

As a result of the calculations for the heat exchanger, Table 8 compares the hand calculations to the software calculations for both the turbine heat transfer and the heat exchanger transfer rate.

Table 9. Comparison between the obtained hand calculations and the same variables as output by the design software to ensure validity.

	Hand Calculated	Software Calculated
$T_{h,i}$	150.09293 °C	150.09 °C
$T_{c,o}$	23.421 °C	23.44 °C
q	111281.6559 W	111954.9578 W

The process that was followed to find the heat exchanger length and the number of tubes required was a series of iterations of the design software to find the specifications that most closely aligned with the desired heat transfer rate. The calculated values were used to find

a heat transfer coefficient, which was then plugged into the software. After that, the tube number, and shell dimensions were fluctuated until the obtained value for q matched the calculated value for q as closely as possible. Figure 20, shown below, illustrates the calculated output from the design software.

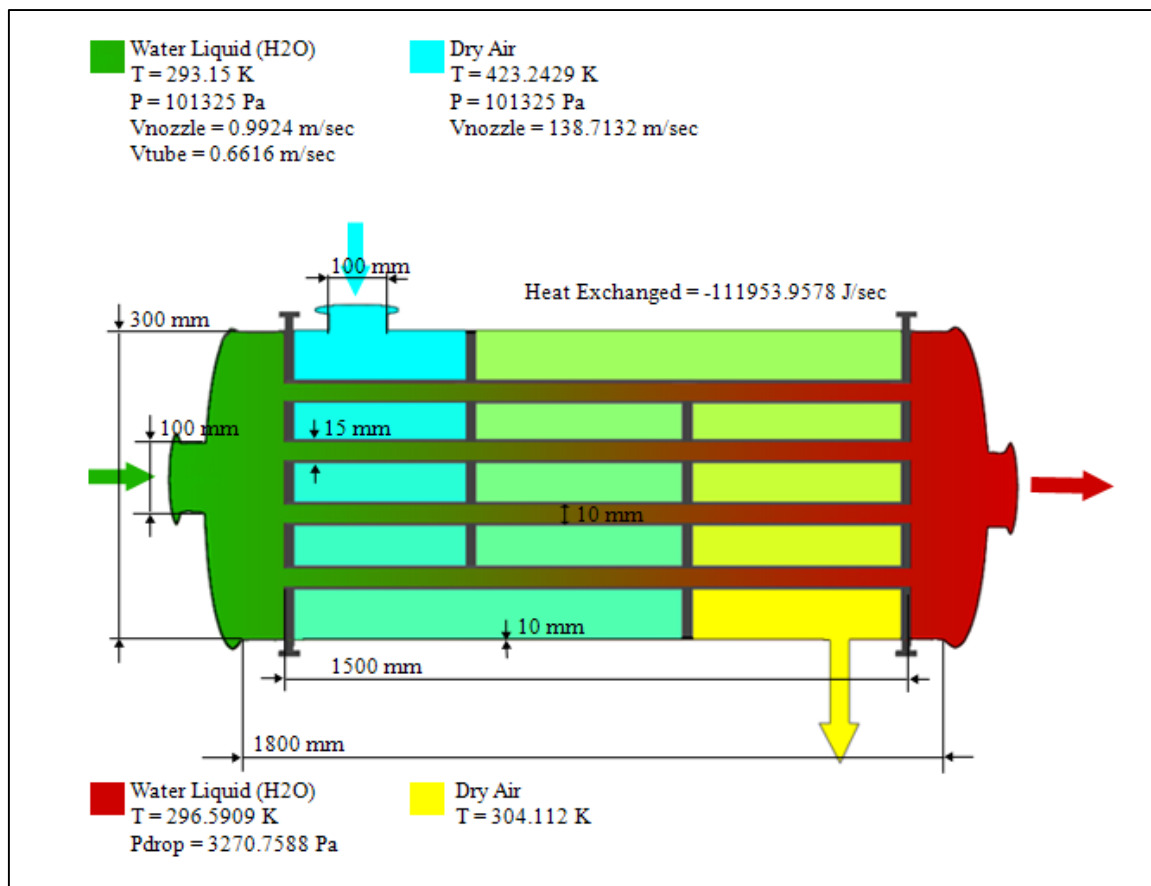


FIG. 20. Graphical illustration of the output from the design software. Calculated values are listed with their respective variables.

The determined specifications for the heat exchanger is a one pass shell and tube design with 300 tubes with a length of 1.5 meters. The shell is 1.8 meters long and .3 meters in diameter. The tubes will be placed into the heat exchanger in a triangular pitch, which increases maintenance costs, but decreases the overall size of the shell. The pitch was designed to be 1.25 times^[14] the outer diameter of the tubes. This value is 18.75 mm. The

full list of output from the design software is shown below in Fig. 21

Conditions for Shell-Side Fluid		Shell-Side (S-S): Fluid Flow	
Fluid	Dry Air	Mass Flow Rate	: 0.91 kg/sec
Mass Flow Rate, kg/sec	0.9105		: 1.09 m ³ /sec
Inlet Temperature, K	423.2429		: 2675.73 scm/h (standard m ³ per hour)
Inlet Pressure, Pa	101325	Inlet Temp-re	: 423.24 K
Density, kg/m ³	1.225	Outlet Temp-re	: 304.11 K
Viscosity, kg/(m*sec)	0	Inlet/Outlet Nozzle Velocity	: 138.71 m/sec
Specific Heat, J/(kg*K)	1006.4	Shell-Side Fluid Properties	
Conditions for Tube-Side Fluid		Fluid	: Dry Air
Fluid	Water Liquid (H2O)	Density	: 1.23 kg/m ³
Mass Flow Rate, kg/sec	7.78	Viscosity	: 1.7894E-005 kg/(m*sec)
Inlet Temperature, K	293.15	Specific Heat	: 1006.40 J/(kg*K)
Inlet Pressure, Pa	101325	Tube-Side (T-S): Fluid Flow	
Density, kg/m ³	998.2	Mass Flow Rate	: 7.78 kg/sec
Viscosity, kg/(m*sec)	0.001		: 0.01 m ³ /sec
Specific Heat, J/(kg*K)	4182		: 28.06 scm/h (standard m ³ per hour)
Heat Exchanger Construction		Velocity in Tube	: 0.66 m/sec
Shell-Side Fluid Nozzle, mm	100	Reynolds Number	: 6578
Shell Diameter, mm	400	Inlet Temp-re	: 293.15 K
Shell Length, mm	1800	Outlet Temp-re	: 296.59 K
Shell Outer Surface, m ²	1.8378	Friction Factor	: 0.0454
Tube-Side Fluid Nozzle, mm	100	Inlet Pressure	: 101325 Pa
Tube Inner Diameter, mm	10	Pressure Drop	: 3270.76 Pa
Tube Outer Diameter, mm	15	Inlet/Outlet Nozzle Velocity	: 0.99 m/sec
Tube Length per Pass, mm	1500	Tube-Side Fluid Properties	
Number of Passes	2	Fluid	: Water Liquid (H2O)
Number of Tubes	300	Density	: 998.20 kg/m ³
Tubes Outer Surface, m ²	21.2058	Viscosity	: 1.0030E-003 kg/(m*sec)
Pipe Roughness, mm	0.1	Specific Heat	: 4182.00 J/(kg*K)
Heat Transfer, W/(K*m ²)	1583.9654	Heat Exchanged between two fluids	
Shell Insulation		Heat Exchanged	: -111954 J/sec
Thermal Conductivity, W/(K*m)	13.4	Thermal Effectiveness of Heat Exchanger	
Thickness, mm	10	Effectiveness	: 0.9157
Heat Transfer, W/(K*m ²)	26		
Ambient Temperature, K	423.2429		
Shell-Side Heater			
Heater Power, W	0		
Number of Tubes			

FIG.21. Complete list of the output from the Kamlex Heat Exchanger software.

The cost associated with implementing the proposed design changes was found to be very minimal. The cost of purchasing a water driven fan, as seen in Fig. 22, is expected to be around \$4326^[15] while the cost of a heat exchanger is expected to be about \$5000.



FIG.22. Water driven pump that could be used in the RCIC heat removal system.^[15]

Since the system will be located in the same room as the pump and turbine the price of piping, valves, and structural modifications are expected to be approximately \$30,000.

V. CONCLUSIONS

V.A. NEUTRONICS

By taking an analytical approach to the method and establishing the governing equations of the physical phenomena that was occurring in the core during decay heat production and using core design data from an existing BWR similar to that of the Fukushima Daiichi site,

a model was able to be created in ORIGEN-ARP. These outputs were then tested and validated using analytical methods based on reactor kinetics theory, decay heat behavior, and radioisotope behavior. The results were then compared numerically to a previously existing numerical approximation to determine their validity. It was discovered that the input decks generated at two different typical BWR burnups, provided realistic outputs that allowed the thermal hydraulics to analyze the behavior and decay heat removal capabilities of the RCIC.

This work could be expanded upon in the future by modifying the core burnups and fuel compositions to model other reactor decay heat removal systems. It can also be expanded upon to create a model that takes into account the spatial distribution throughout the core to potentially detect problem areas and hot channels that may result from the decay heat generation during a station blackout.

V.B. THERMAL HYDRAULICS

From the output of the initial RELAP5 input deck it was seen that there was an adequate supply of coolant to cool the core for at least 19 hours. This is a very important result because it means for the first 19 hours, the problems associated with drawing a suction from the suppression pool can be neglected. It was also found that the system requires being turned off and on multiple times during this time period. Although it was not within the scope of this project, it may cause concern since the operation of some of the controls may have to be done by the station battery power which is limited.

With the addition of a heat exchanger it was found that, since the required flow of the modifications was very minimal in comparison with the total flow provided by the RCIC system, the failure caused by room temperature can be eliminated. This is a very good result. It is an indication that the heat exchanger is an answer to the problem of removing the heat buildup in the room. Thus, it is suggested that BWR power plants make this modification to their RCIC system to allow them to take credit for the safety system being capable for cooling the core during a station blackout, during a 19 hour window.

V.C. SYSTEM MODIFICATIONS

With the addition of the heat exchanger, it was found that all of the heat emitted from the turbine can be transferred out of the system. In order to integrate this heat exchanger into the current RCIC system, a T-pipe needs to be connected to the feed line that runs from the pump to the reactor core. The diameter of this T-pipe needs to be 100 mm to be compatible with the proposed heat exchanger design. A globe valve is also recommended between the feed line and the heat exchanger in order to isolate the system for required maintenance, such as possible leaks in the tubes.

The water flow rate that is required to operate the fan and obtain the required heat transfer rate is small enough with respect to the overall water mass flow rate that the addition of this equipment into the overall RCIC system will negligibly effect the performance of the RCIC system in regards to decreasing water mass flow rate. Therefore, the benefit of the prevention of the turbine room from overheating with no appreciable loss in coolant mass flow rate is extremely attractive.

A conservative cost estimate associated with implementing this design would be around \$39,326. Considering the costs of operating a power plant from day to day this is a very low cost for the amount of safety that it will provide. Also, since the modifications are minimal it is expected that the design can be implemented within the time frame of a regular refueling outage. The recommendation of this report is that BWR power plants install this relatively simple modification into their RCIC systems to increase the operation time of their systems.

REFERENCES

1. *The Effects of Aging on BWR Core Isolation Cooling Systems*, Fresco, U.S. Nuclear Regulatory Commission, (October 1994).
2. *Fukushima Daiichi: American Nuclear Society Committee Report, Appendix F*. American Nuclear Society.
http://fukushima.ans.org/inc/Fukushima_Appendix_F.pdf. (Jun. 2012).
3. *Facility Description and Safety Analysis Report, Unit 1 Volume 1*, Northern States Power Company (1965).
4. *The Condensate Storage Tanks At Fukushima Daiichi*, Simply Info, <http://www.simplyinfo.org/?p=3838>. (Nov. 2011)
5. *Fundamentals of Nuclear Reactor Physics*. E.E. Lewis. Elsevier. (2008)
6. *WolframAlpha Computational Knowledge Engine*. Wolfram Alpha LLC, <http://www.wolframalpha.com/input/?i=Iodine+135+xenon+135>. (2013)
7. *Reactor Pool Calorimetrics, Laboratory 09*, W. D. Reece, NUEN 405 Class Notes, Department of Nuclear Engineering, Texas A&M University (2011).
8. *SCALE: Getting Started with Scale 6.1*, Oakridge National Lab, (2011).
9. *Fundamentals of Heat and Mass Transfer, Seventh Edition*, Theodore L. Bergman, Adrienne S. Lavine, Frank P. Incropera, David P. Dewitt. (2007)
10. *Advantages and Disadvantages of Shell and Tube & Plate type Heat Exchangers*, Jabelu Firoz, (2013)
11. *KamLex Shell-and-Tube Heat Exchanger 1.1*, KamLex, (2007)
12. *Technical Report, Toshiba Corporation*. South Texas Projects Units 3&4 RCIC Turbine-Pump, (Mar. 2010).

13. *Chun Hao Axial Flow CSZ-380 Explosion Proof Exhaust Fan*, Qingdao
http://www.alibaba.com/product-gs/385596916/Oil_tanker_water_power_gas_free.html
14. *How to Design a Shell-and-Tube Heat Exchanger*, R. Shankar Subramanian, (2008)
15. Texas Pneumatic Tools, *INC.*, <http://www.airtools.com/catalog/air-movement/fans/tx-wd16.aspx> (2013)

APPENDIX

ORIGEN-ARP 20 GWd/MTU

```
'This SCALE input file was generated by
'OrigenArp Version 6.1 Compiled on Thu Oct 7 11:31:00 2010
=arp
ge7x7-0
2.03
2
180
185
13.581188
13.581188
1
1
0.75
ft33f001
end
#origens
0$$ a4 33 a11 71 e t
ge7x7-0
3$$ 33 a3 1 27 a16 2 a33 18 e t
35$$ 0 t
56$$ 10 10 a6 3 a10 0 a13 4 a15 3 a18 1 e
57** 0 a3 1e-05 0.4931507 e
95$$ 0 t
Cycle 1 -20gwd4-21-13
108.1643 MTU
58** 1469 1469 1469 1469 1469 1469 1469 1469 1469 1469
60** 18 36 54 72 90 108 126 144 162 180
66$$ a1 2 a5 2 a9 2 e
73$$ 922340 922350 922360 922380
74** 19542.05 2195736 10100.38 1.059389e+08
75$$ 2 2 2 2
t
ge7x7-0
3$$ 33 a3 2 27 a33 18 e t
35$$ 0 t
56$$ 10 10 a10 10 a15 3 a18 1 e
57** 180 a3 1e-05 0.5068493 e
95$$ 0 t
Cycle 2 -20gwd4-21-13
108.1643 MTU
58** 1469 1469 1469 1469 1469 1469 1469 1469 1469
60** 198.5 217 235.5 254 272.5 291 309.5 328 346.5 365
66$$ a1 2 a5 2 a9 2 e t
```

54\$\$ a8 1 a11 0 e
 56\$\$ a2 7 a6 1 a10 10 a14 3 a15 3 a17 2 e
 57** 0 a3 1e-05 e
 95\$\$ 0 t
 Cycle 3 Down - 20gwd4-21-13
 108.1643 MTU
 60** 0.001 0.003 0.01 0.03 0.1 0.3 0.5
 61** f0.05
 65\$\$
 'Gram-Atoms Grams Curies Watts-All Watts-Gamma
 3z 1 0 0 3z 3z 3z 6z
 3z 1 0 0 3z 3z 3z 6z
 3z 1 0 0 3z 3z 3z 6z
 81\$\$ 2 0 26 1 a7 200 e
 82\$\$ 2 2 2 2 2 2 2 e
 83**
 1.000000e+07 8.000000e+06 6.500000e+06 5.000000e+06 4.000000e+06
 3.000000e+06 2.500000e+06 2.000000e+06 1.660000e+06 1.330000e+06
 1.000000e+06 8.000000e+05 6.000000e+05 4.000000e+05 3.000000e+05
 2.000000e+05 1.000000e+05 5.000000e+04 1.000000e+04 e
 84**
 2.000000e+07 8.1873000e+06 6.4340000e+06 4.8000000e+06
 3.0000000e+06 2.4790000e+06 2.3540000e+06 1.8500000e+06 1.4000000e+06
 9.0000000e+05 4.0000000e+05 1.0000000e+05 2.5000000e+04 1.7000000e+04
 3.0000000e+03 5.5000000e+02 1.0000000e+02 3.0000000e+01 1.0000000e+01
 8.1000000e+00 6.0000000e+00 4.7500000e+00 3.0000000e+00 1.7700000e+00
 1.0000000e+00 6.2500000e-01 4.0000000e-01 3.7500000e-01 e
 t
 56\$\$ 0 0 a10 1 e t
 56\$\$ 0 0 a10 2 e t
 56\$\$ 0 0 a10 3 e t
 56\$\$ 0 0 a10 4 e t
 56\$\$ 0 0 a10 5 e t
 56\$\$ 0 0 a10 6 e t
 56\$\$ 0 0 a10 7 e t
 54\$\$ a8 1 a11 0 e
 56\$\$ a2 4 a6 1 a10 7 a14 3 a15 3 a17 2 e
 57** 0.5 a3 1e-05 e
 95\$\$ 0 t
 Case 4
 108.1643 MTU
 60** 1.5 4.5 13.5 24
 61** f0.05
 65\$\$
 'Gram-Atoms Grams Curies Watts-All Watts-Gamma
 3z 1 0 0 3z 3z 3z 6z
 3z 1 0 0 3z 3z 3z 6z
 3z 1 0 0 3z 3z 3z 6z
 81\$\$ 2 0 26 1 a7 200 e
 82\$\$ 2 2 2 2 e
 83**
 1.000000e+07 8.000000e+06 6.500000e+06 5.000000e+06 4.000000e+06
 3.000000e+06 2.500000e+06 2.000000e+06 1.660000e+06 1.330000e+06
 1.000000e+06 8.000000e+05 6.000000e+05 4.000000e+05 3.000000e+05
 2.000000e+05 1.000000e+05 5.000000e+04 1.000000e+04 e
 84**

2.000000e+07 8.187300e+06 6.434000e+06 4.800000e+06
3.000000e+06 2.479000e+06 2.354000e+06 1.850000e+06 1.400000e+06
9.000000e+05 4.000000e+05 1.000000e+05 2.500000e+04 1.700000e+04
3.000000e+03 5.500000e+02 1.000000e+02 3.000000e+01 1.000000e+01
8.100000e+00 6.000000e+00 4.750000e+00 3.000000e+00 1.770000e+00
1.000000e+00 6.250000e-01 4.000000e-01 3.750000e-01 e
t
56\$\$ 0 0 a10 1 e t
56\$\$ 0 0 a10 2 e t
56\$\$ 0 0 a10 3 e t
56\$\$ 0 0 a10 4 e t
54\$\$ a8 1 a11 0 e
56\$\$ a2 2 a6 1 a10 4 a14 3 a15 3 a17 2 e
57** 24 a3 1e-05 e
95\$\$ 0 t
Case 5
108.1643 MTU
60** 30 72
61** f0.05
65\$\$
'Gram-Atoms Grams Curies Watts-All Watts-Gamma
3z 1 0 0 3z 3z 3z 6z
3z 1 0 0 3z 3z 3z 6z
3z 1 0 0 3z 3z 3z 6z
81\$\$ 2 0 26 1 a7 200 e
82\$\$ 2 2 e
83**
1.000000e+07 8.000000e+06 6.500000e+06 5.000000e+06 4.000000e+06
3.000000e+06 2.500000e+06 2.000000e+06 1.660000e+06 1.330000e+06
1.000000e+06 8.000000e+05 6.000000e+05 4.000000e+05 3.000000e+05
2.000000e+05 1.000000e+05 5.000000e+04 1.000000e+04 e
84**
2.000000e+07 8.187300e+06 6.434000e+06 4.800000e+06
3.000000e+06 2.479000e+06 2.354000e+06 1.850000e+06 1.400000e+06
9.000000e+05 4.000000e+05 1.000000e+05 2.500000e+04 1.700000e+04
3.000000e+03 5.500000e+02 1.000000e+02 3.000000e+01 1.000000e+01
8.100000e+00 6.000000e+00 4.750000e+00 3.000000e+00 1.770000e+00
1.000000e+00 6.250000e-01 4.000000e-01 3.750000e-01 e
t
56\$\$ 0 0 a10 1 e t
56\$\$ 0 0 a10 2 e t
56\$\$ f0 t
end
=opus
LIBUNIT=33
TYPARAMS=NUCLIDES
UNITS=GPERCM
SYMNUC=I-135 Xe-135 end
NRANK=2
LIBTYPE=FISS
VFUEL=108956
TIME=HOURS
NPOSITION=1 2 3 4 5 6 7 8 9 10 11 12 13 end
end
#shell
copy ft71f001 "W:\SCALE\cbanoout\Final\20gwd421.f71"

del ft71f001
end

ORIGEN-ARP 30GWD/MTU

'This SCALE input file was generated by
'OrigenArp Version 6.1 Compiled on Thu Oct 7 11:31:00 2010

=arp
ge7x7-0
2.03
2
180
185
13.581189
13.581189
1
1
0.7332
ft33f001
end
#origens
0\$\$ a4 33 a11 71 e t
ge7x7-0
3\$\$ 33 a3 1 27 a16 2 a33 18 e t
35\$\$ 0 t
56\$\$ 10 10 a6 3 a10 0 a13 4 a15 3 a18 1 e
57** 0 a3 1e-05 0.4931507 e
95\$\$ 0 t
Cycle 1 Part 1 -30gwd421
108.1643 MTU
58** 1469 1469 1469 1469 1469 1469 1469 1469 1469 1469
60** 18 36 54 72 90 108 126 144 162 180
66\$\$ a1 2 a5 2 a9 2 e
73\$\$ 922340 922350 922360 922380
74** 19542.05 2195736 10100.38 1.059389e+08
75\$\$ 2 2 2 2

t

ge7x7-0

3\$\$ 33 a3 2 27 a33 18 e t

35\$\$ 0 t

56\$\$ 10 10 a10 10 a15 3 a18 1 e

57** 180 a3 1e-05 0.5068493 e

95\$\$ 0 t

Cycle 2 Part 2 -30gwd421

108.1643 MTU

58** 1469 1469 1469 1469 1469 1469 1469 1469 1469 1469

60** 198.5 217 235.5 254 272.5 291 309.5 328 346.5 365

66\$\$ a1 2 a5 2 a9 2 e t

54\$\$ a8 1 a11 0 e

56\$\$ a2 7 a6 1 a10 10 a14 3 a15 3 a17 2 e

57** 0 a3 1e-05 e

95\$\$ 0 t

Cycle 2 Down - 30gwd421

108.1643 MTU

60** 0.001 0.003 0.01 0.03 0.1 0.3 0.5

61** f0.05

65\$\$

'Gram-Atoms Grams Curies Watts-All Watts-Gamma

3z 1 0 0 3z 3z 3z 6z

3z 1 0 0 3z 3z 3z 6z

3z 1 0 0 3z 3z 3z 6z

81\$\$ 2 0 26 1 a7 200 e

82\$\$ 2 2 2 2 2 2 2 e

83**

1.000000e+07 8.000000e+06 6.500000e+06 5.000000e+06 4.000000e+06

3.000000e+06 2.500000e+06 2.000000e+06 1.660000e+06 1.330000e+06

1.000000e+06 8.000000e+05 6.000000e+05 4.000000e+05 3.000000e+05

2.000000e+05 1.000000e+05 5.000000e+04 1.000000e+04 e

84**

2.000000e+07 8.187300e+06 6.434000e+06 4.800000e+06

3.000000e+06 2.479000e+06 2.354000e+06 1.850000e+06 1.400000e+06

9.000000e+05 4.000000e+05 1.000000e+05 2.500000e+04 1.700000e+04

3.000000e+03 5.500000e+02 1.000000e+02 3.000000e+01 1.000000e+01

8.1000000e+00 6.0000000e+00 4.7500000e+00 3.0000000e+00 1.7700000e+00
1.0000000e+00 6.2500000e-01 4.0000000e-01 3.7500000e-01 e

t

56\$\$ 0 0 a10 1 e t

56\$\$ 0 0 a10 2 e t

56\$\$ 0 0 a10 3 e t

56\$\$ 0 0 a10 4 e t

56\$\$ 0 0 a10 5 e t

56\$\$ 0 0 a10 6 e t

56\$\$ 0 0 a10 7 e t

54\$\$ a8 1 a11 0 e

56\$\$ a2 4 a6 1 a10 7 a14 3 a15 3 a17 2 e

57** 0.5 a3 1e-05 e

95\$\$ 0 t

Case 4

108.1643 MTU

60** 1.5 4.5 13.5 24

61** f0.05

65\$\$

'Gram-Atoms Grams Curies Watts-All Watts-Gamma

3z 1 0 0 3z 3z 3z 6z

3z 1 0 0 3z 3z 3z 6z

3z 1 0 0 3z 3z 3z 6z

81\$\$ 2 0 26 1 a7 200 e

82\$\$ 2 2 2 2 e

83**

1.0000000e+07 8.0000000e+06 6.5000000e+06 5.0000000e+06 4.0000000e+06

3.0000000e+06 2.5000000e+06 2.0000000e+06 1.6600000e+06 1.3300000e+06

1.0000000e+06 8.0000000e+05 6.0000000e+05 4.0000000e+05 3.0000000e+05

2.0000000e+05 1.0000000e+05 5.0000000e+04 1.0000000e+04 e

84**

2.0000000e+07 8.1873000e+06 6.4340000e+06 4.8000000e+06

3.0000000e+06 2.4790000e+06 2.3540000e+06 1.8500000e+06 1.4000000e+06

9.0000000e+05 4.0000000e+05 1.0000000e+05 2.5000000e+04 1.7000000e+04

3.0000000e+03 5.5000000e+02 1.0000000e+02 3.0000000e+01 1.0000000e+01

8.1000000e+00 6.0000000e+00 4.7500000e+00 3.0000000e+00 1.7700000e+00

1.0000000e+00 6.2500000e-01 4.0000000e-01 3.7500000e-01 e

```

t
56$$ 0 0 a10 1 e t
56$$ 0 0 a10 2 e t
56$$ 0 0 a10 3 e t
56$$ 0 0 a10 4 e t
54$$ a8 1 a11 0 e
56$$ a2 2 a6 1 a10 4 a14 3 a15 3 a17 2 e
57** 24 a3 1e-05 e
95$$ 0 t
Case 5
108.1643 MTU
60** 30 72
61** f0.05
65$$
'Gram-Atoms Grams Curies Watts-All Watts-Gamma
3z 1 0 0 3z 3z 3z 6z
3z 1 0 0 3z 3z 3z 6z
3z 1 0 0 3z 3z 3z 6z
81$$ 2 0 26 1 a7 200 e
82$$ 2 2 e
83**
1.000000e+07 8.000000e+06 6.500000e+06 5.000000e+06 4.000000e+06
3.000000e+06 2.500000e+06 2.000000e+06 1.660000e+06 1.330000e+06
1.000000e+06 8.000000e+05 6.000000e+05 4.000000e+05 3.000000e+05
2.000000e+05 1.000000e+05 5.000000e+04 1.000000e+04 e
84**
2.000000e+07 8.187300e+06 6.434000e+06 4.800000e+06
3.000000e+06 2.479000e+06 2.354000e+06 1.850000e+06 1.400000e+06
9.000000e+05 4.000000e+05 1.000000e+05 2.500000e+04 1.700000e+04
3.000000e+03 5.500000e+02 1.000000e+02 3.000000e+01 1.000000e+01
8.100000e+00 6.000000e+00 4.750000e+00 3.000000e+00 1.770000e+00
1.000000e+00 6.250000e-01 4.000000e-01 3.750000e-01 e
t
56$$ 0 0 a10 1 e t
56$$ 0 0 a10 2 e t
56$$ f0 t
end

```



```

=opus
LIBUNIT=33
TYPARAMS=NUCLIDES
UNITS=GPERCM
SYMNUC=I-135 Xe-135 end
NRANK=2
LIBTYPE=ALL
VFUEL=108956
TIME=HOURS
NPOSITION=1 2 3 4 5 6 7 8 9 10 11 12 13 end
end
#shell
copy ft71f001 "W:\SCALE\cbanout\Final\30gwd421.f71"
del ft71f001
end

```

RELAP5-3D INPUT DECK

```

=BWR-RCIC

100 new transnt
*
102 british british
105 5.0 6.0 5000.0
110 nitrogen
*****
*           time step cards           *
*****
*
201 10000.0 1.0-7 0.10 7 10 2000 40000
*
*****
*                               *
*           minor edit variables       *

```

* *

*
301 p 345010000
304 voidg 345010000
305 voidg 335060000
308 httmp 336000609
*

*TRIP CARDS

*501 voidf 315010000 ge null 0 0.85 n
501 p 315010000 le null 0 0.97 n
502 time 0 ge timeof 501 1500.0 n
503 p 315010000 le null 0 1860.0 l
*

120 345010000 -1.041645 h2o primary

*BLOWDOWN

3900000 bl-down sngljun
3900101 345010000 391000000 0.0 0.06 0.06 0100
3900201 1 30464.55 0.0 0.0
3900113 0.0 0.0 0.0 0.0
3910000 bl-tank snglvol
* A L V AA IA EC Eps H.Dia lpybfe
3910101 1.e7 15.0 0.0 0.0 0.0 0.0 0.000046 0.0 00000
* ebt P(pa) T(K) e
3910200 100 14.5 98.7

* hydrodynamic components *

*
3800000 up-ihl sngljun
3800101 345010000 100000000 0.0 0.06 0.06 0100
3800201 1 30464.55 0.0 0.0
3800113 0.0 0.0 0.0 0.0
*

*

1000000 ihl pipe
1000001 2
1000101 15.420 1
1000102 13.761 2
1000301 3.339 1
1000302 4.362 2
1000501 22.0 2
1000601 0.0 2
1000801 0.0 2.558 1
1000802 0.0 2.417 2
1001001 00 2
1001101 0000 1
1001201 3 2245.1 589.25 0.0 0 0 1
1001202 3 2242.6 589.23 0.0 0 0 2
1001300 1
1001301 30464.55 0.0 0.0 1

*

* TURBINE

1150000 corev valve
1150101 102010000 103000000 0.0002 1.0 1.0 1 1.0 1.0 1.0
1150201 1 100.0 0.0
1150300 trpvlv
1150301 520

* SUPPRESSION POOL

1030000 BDWNTNK snglvol
* A L V AA IA EC Eps H.Dia lpbfe
1030101 1.e6 500.0 0.0 0.0 0.0 0.0 0.000046 0.0 00000

* ebt P(pa) T(K) e

1030200 3 14.5 98.7

* CONDENSATE STORAGE TANK

1040000 CSST snglvol
* A L V AA IA EC Eps H.Dia lpbfe
1040101 120 5.0 0.0 0.0 0.0 0.0 0.000046 0.0 00000

```

*   ebt P(pa) T(K)   e
1040200 100 14.5 98.7
*
1050000 CSSTJUNC  sngljun
1050101 104010000 112000000 0.0  0.9  0.9  0100
1050113 0.0 0.0 -0.41192 -0.28656
1050201 1 30464.55 0.0 0.0
*
1120000 iclps pipe
1120001 5
1120101 15.723 5
1120301 4.601 1
1120302 4.768 2
1120303 6.709 3
1120304 4.219 4
1120305 6.938 5
1120501 120.0 5
1120601 -69.3008 1
1120602 -90.0 2
1120603 -39.5393 3
1120604 0.0 4
1120605 40.4363 5
1120701 -4.304 1
1120702 -4.768 2
1120703 -4.271 3
1120704 0.0 4
1120705 4.5 5
1120801 0.0 2.583 5
1120901 0.075 0.075 1
1120902 0.069 0.069 4
1121001 00 5
1121101 0000 4
1121201 3 2205.3 529.71 0.0 0 0 1
1121202 3 2206.1 529.72 0.0 0 0 2
1121203 3 2206.9 529.72 0.0 0 0 3
1121204 3 2207.0 529.72 0.0 0 0 4
1121205 3 2205.5 529.72 0.0 0 0 5

```

1121300 1
 1121301 30464.55 0.0 0.0 4
 *
 1130000 ipump pump
 1130101 0.0 5.812 168. 225.0 90.0 5.812 0
 1130108 112010000 15.723 0.069 0.069 0000
 1130109 114000000 12.3741 0.0 0.0 0000
 1130200 3 2246.0 529.93 0.0
 1130201 1 30464.55 0.0 0.0
 1130202 1 30464.55 0.0 0.0
 1130301 -2 0 -2 -1 -1 502 0
 1130302 1189. 1.0057 265500. 277. 94800. 246000. 62.4
 1130303 0. 0. 2400. 0.0 0.0
 *
 *
 1133001 0 0.0,0.0 0.1,0.0 0.15,0.05 0.24,0.8 0.3,0.96 0.4,0.98
 1133002 0.6,0.97 0.8,0.9 0.9,0.8 0.96,0.5 1.0,0.0
 *
 1133101 0 0.0,0.0 0.1,0.0 0.15,0.05 0.24,0.56 0.8,0.56 0.96,0.45
 1133102 1.0,0.0
 *
 *
 1140000 iclpd pipe
 1140001 1
 1140101 12.3741 1
 1140301 0.0 1
 1140401 93. 1
 1140501 225. 1
 1140601 0.0 1
 1140801 0.0 2.292 1
 1141001 10 1
 1141201 3 2282.7 530.07 0. 0 0 1
 *
 *
 1160000 iclpd branch
 1160001 2 1
 1160101 12.3741 7.53905 0.0 225.0 0.0 0.0 0.0 2.292 00

1160191 0.0 2.292 0.0 0.0 00000 0 0 2.292
1160200 3 2280.7 530.07
1161101 114010000 116000000 12.3741 0.14 0.14 0000
1162101 116010000 118000000 12.3741 0.0 0.0 0000
1161201 30464.55 0.0 0.0
1162201 30464.55 0.0 0.0

*

*

1180000 iclpd pipe
1180001 2
1180101 12.3741 1
1180102 0.0 2
1180301 7.53905 1
1180302 9.7632 2
1180401 0.0 1
1180402 143.8062 2
1180501 225.0 1
1180502 225.0 2
1180601 0.0 2
1180801 0.0 2.292 1
1180802 0.0 2.50 2
1180901 0.05 0.05 1
1181001 00 2
1181101 0000 1
1181201 3 2280.4 530.07 0. 0 0 1
1181202 3 2283.6 530.08 0. 0 0 2
1181300 1
1181301 30464.55 0.0 0.0 1

*

*

3850000 icl-dwnc sngljun
3850101 118010000 300000000 0.0 0.9 0.9 0100
3850113 0.0 0.0 -0.41192 -0.28656
3850201 1 30464.55 0.0 0.0

*

```

* vessel *
*****
*
* inlet annulus - branch (300),branch (305),pipe (310)
*
* branch (300) - cold leg connection
*
3000000 inlet branch
3000001 2 1
3000101 19.7945 0.0 41.23860 0.0 -90.0
3000102 -2.08329 0.0 1.3764 00
3000200 3 2275.3 530.09
3003101 300010000 305000000 19.7945 0.000 0.000 0000
3004101 300000000 310000000 19.7945 0.0 0.0 0000
3003201 40000. 0.0 0.0
3004201 100. 0.0 0.0
*
* branch (305) inlet annulus lower volume
*
3050000 inletlow branch
3050001 2 1
3050101 29.3518 0.0 66.0416 0.0 -90.0
3050102 -2.24999 0.0 1.0675 00
3050200 3 2281.1 530.11
3051101 305010000 315000000 26.7199 0.0636 0.0217 0000
3052101 305010000 320000000 3.0 50. 50.0000
3052113 0.0 0.0 -1.47829 0.0
3051201 40000. 0.0 0.0
3052201 100.0 0.0 0.0
*
* pipe (310) inlet annulus top volume
*
3100000 inlettop pipe
3100001 4
3100101 19.7945 1
3100102 32.6417 2
3100103 15.4795 3

```

3100104	15.0903	4						
3100201	32.6417	2						
3100202	15.0903	3						
3100301	0.0	4						
3100401	41.2386	1						
3100402	80.2442	2						
3100403	38.0538	3						
3100404	22.63545	4						
3100501	0.0	4						
3100601	90.0	4						
3100701	2.0833	1						
3100702	2.4583	2						
3100703	2.4583	3						
3100704	1.1978	4						
3100801	0.0	1.3764	1					
3100802	0.0	1.5417	3					
3100803	0.0	0.7083	4					
3100901	0.0	0.0	1					
3100902	0.0	0.0	2					
3100903	6.176e5	6.176e5	3					
3101001	00	4						
3101101	0000	2						
3101102	0000	3						
3101201	3	2284.1	530.09	0.0	0.0	1		
3101202	3	2283.3	530.03	0.0	0.0	2		
3101203	3	2282.5	530.01	0.0	0.0	3		
3101204	3	2256.2	529.99	0.0	0.0	4		
3101300	1							
3101301	100.	0.0	0.0	3				
*								
* downcomer - pipe (315)								
*								
3150000	dcomer	annulus						
3150001	8							
3150101	26.7199	8						
3150301	0.0	8						
3150401	57.0560	1						

3150402	58.3376	5		
3150403	66.9681	6		
3150404	38.9870	7		
3150405	89.0654	8		
3150501	0.0	8		
3150601	-90.0	8		
3150701	-2.1353	1		
3150702	-2.18328	5		
3150703	-2.50627	6		
3150704	-1.45900	7		
3150705	-3.33328	8		
3150801	0.0	0.630	8	
3150901	0.0	0.0	1	
3150902	0.0	0.0000	3	
3150903	0.0	0.0	4	
3150904	0.0	0.0	5	
3150905	0.0256	0.0558	6	
3150906	0.0	0.0	7	
3151001	00	8		
3151101	0000	7		
3151201	3	2280.6	530.11	0.0 0 0 1
3151202	3	2281.2	530.11	0.0 0 0 2
3151203	3	2281.8	530.12	0.0 0 0 3
3151204	3	2282.4	530.12	0.0 0 0 4
3151205	3	2283.0	530.12	0.0 0 0 5
3151206	3	2283.6	530.13	0.0 0 0 6
3151207	3	2284.0	530.13	0.0 0 0 7
3151208	3	2284.7	530.13	0.0 0 0 8
3151300	1			
3151301	40365.9	0.0	0.0	7

*

* downcomer bypass - pipe (320)

*

3200000 dcbypass pipe

3200001 6

3200101 18.6736 6

3200201 2.0 5

3200301 2.1353,1 2.18328,5 2.50627,6
3200401 0.0 6
3200501 0.0 6
3200601 -90.0 6
3200701 -2.1353 1
3200702 -2.18328 5
3200703 -2.50627 6
3200801 0.0 0.9591 6
3200901 0.0 0.0 1
3200902 0.0 0.0 2
3200903 0.0 0.0 3
3200904 0.0 0.0 4
3200905 0.0 0.0 5
3201001 00 6
3201101 0100 5
3201201 3 2283.1 530.37 0.0 0 0 1
3201202 3 2283.6 530.60 0.0 0 0 2
3201203 3 2284.2 530.77 0.0 0 0 3
3201204 3 2284.7 530.89 0.0 0 0 4
3201205 3 2285.3 530.96 0.0 0 0 5
3201206 3 2285.9 531.04 0.0 0 0 6
3201300 1
3201301 100. 0.0 0.0 5
*
* lower plenum - branch (322),snglvol (323),snglvol (325),branch (330)
*
* branch (322)
*
3220000 lplenuml branch
3220001 3 1
3220101 130.0 0.0 236.0 0.0 -90.0
3220102 -1.81537 0.0 2.30 00
3220200 3 2288.6 530.15
3221101 315010000 322000000 26.7199 0.3759 0.1400 0000
3221113 0.0 0.0 -1.03959 0.0
3222101 322000000 325000000 49.6 0.1769 0.17690 0100
3223101 322010000 323000000 130.0 0.0 0.0 0000

3221201 40000.0 0.0 0.0
 3222201 40000.0 0.0 0.0
 3223201 0.0 0.0 0.0
 *
 * snglvol (323)
 *
 3230000 lplenum1 snglvol
 3230101 130.0 0.0 236.0 0.0 -90.0
 3230102 -1.81537 0.0 2.30 00
 3230200 3 2289.2 530.0
 *
 * snglvol (325)
 *
 3250000 lplenumm snglvol
 3250101 91.20 0.0 304.0 0.0 90.0
 3250102 3.3333 0.0 1.15 00
 3250200 3 2286.8 530.15
 *
 * branch (330)
 *
 3300000 lplenum2 branch
 3300001 3 1
 3300101 112.4 0.0 164.0 0.0 90.0
 3300102 1.4590 0.0 3.2 00
 3300200 3 2284.6 530.15
 3301101 320010000 330010000 3.0 120. 120. 0000
 3301113 0.0 0.0 0.51548 0.0
 3302101 325010000 330000000 54.2000 0.9658 0.9658 0100
 3303101 330010000 335000000 31.8000 1.2163 1.2163 0100 *1.2163
 3301201 100. 0.0 0.0
 3302201 40000. 0.0 0.0
 3303201 40000. 0.0 0.0
 *
 * core -pipe (335)
 *
 3350000 core pipe
 3350001 6

3350101 53.65 6
3350201 51.20028 5
3350301 0.0 6
3350401 133.8535 1
3350402 116.6042 5
3350403 114.0409 6
3350501 0.0 6
3350601 90.0 6
3350701 2.50627 1
3350702 2.18329 5
3350703 2.1353 6
3350801 0.0 0.04418 6
3350901 0.8077 0.8077 1 *0.8077
3350902 0.8077 0.8077 2
3350903 0.8077 0.8077 3
3350904 0.8077 0.8077 4
3350905 0.8077 0.8077 5
3351001 00 6
3351101 0000 5
3351201 3 2277.3 539.15 0.0 0 0 1
3351202 3 2274.6 552.07 0.0 0 0 2
3351203 3 2271.9 564.89 0.0 0 0 3
3351204 3 2269.2 577.15 0.0 0 0 4
3351205 3 2266.5 587.27 0.0 0 0 5
3351206 3 2263.7 589.42 0.0 0 0 6
3351300 1
3351301 40554.4 0.0 0.0 5
*
* core to upper plenum connection -single junction (336)
*
3360000 coretoup sngljun
3360101 335010000 340000000 51.8004 2.7221 2.7221 0000 *2.7221
3360201 1 40554.4 0.0 0.0
*
* upper plenum - snglvol (340),branch (345),pipe (350)
*
* snglvol (340)

```

*
3400000 upvol1  snglvol
3400101 113.0  0.0  254.25  0.0  90.0
3400102 2.2499  0.0  1.67  0.0
3400200 3      2259.4  589.41
*
* branch (345)
*
3450000 upvol2  branch
3450001 2      1
3450101 113.0  0.0  235.4129  0.0  90.0
3450102 2.08329  0.0  1.67  00
3450200 3      2258.7  589.32
3451101 340010000 345000000 113.0  0.0  0.0  0000
3452101 350010000 345010000 113.0  0.0  0.0  0000
3451201 40554.4  0.0  0.0
3452201 65.0  0.0  0.0
3450181 0.0  6.166667  0.0  1.67  000000  0.  0.  0.
3450191 0.0  6.166667  0.0  1.67  000000  0.  0.  0.
*
* pipe (350)
*
3500000 upvol3  pipe
3500001 4
3500101 113.0  1
3500102 113.0  2
3500103 113.0  3
3500104 113.0  4
3500301 0.0  4
3500401 135.3514  1
3500402 277.7879  2
3500403 277.7879  3
3500404 235.41294  4
3500501 0.0  4
3500601 -90.0  4
3500701 -1.1978  1
3500702 -2.4583  2

```

3500703 -2.4583 3
3500704 -2.0833 4
3500801 0.0 1.67 4
3500901 0.0 0.0 1
3500902 0.0 0.0 2
3500903 0.0 0.0 3
3501001 00 4
3501101 0000 3
3501201 3 2256.2 589.32 0.0 0 0 1
3501202 3 2256.8 589.32 0.0 0 0 2
3501203 3 2257.6 589.32 0.0 0 0 3
3501204 3 2258.4 589.32 0.0 0 0 4
3501300 1
3501301 100. 0.0 0.00 3
*
* upper head - branch (355),pipe (356)
*
3550000 upperhd1 branch
3550001 3 1
3550101 70.9 0.0 122.25 0.0 -90.0
3550102 -1.3485 0.0 1.3 00
3550200 3 2255.8 500.
3551101 310010000 355010000 14. 0.5 0.5 0100
3551113 0.0 0.0 1.40771 0.0
3552101 355010000 350000000 70.9 251.34 251.34 0000
3553101 356010000 355000000 70.9 0.0 0.0 0000
3551201 100. 0.0 0.0
3552201 100. 0.0 0.0
3553201 0.0 0.0 0.0
*
* pipe (356)
*
3560000 upperhd2 pipe
3560001 3
3560101 70.9 3
3560301 0.0 3
3560401 122.25 3

```

3560501 0.0 3
3560601 -90.0 3
3560701 -1.3485 3
3560801 0.0 1.3 3
3560901 0.0 0.0 2
3561001 00 3
3561101 0000 2
3561201 3 2254.4 500. 0.0 0 0 1
3561202 3 2254.9 500. 0.0 0 0 2
3561203 3 2255.3 500. 0.0 0 0 3
3561300 1
3561301 0.0 0.0 0.0 2

```

* vessel heat slabs *

*

* inlet annulus

*

```

13000000 6 3 2 1 7.125
13000100 0 1
13000101 2 8.0208
13000201 5 2
13000301 0.0 2
13000401 530.0 3
13000501 305010000 0 1 1 2.250 1
13000502 300010000 0 1 1 2.08329 2
13000503 310010000 0 1 1 2.08333 3
13000504 310020000 0 1 1 2.45833 4
13000505 310030000 0 1 1 2.45833 5
13000506 310040000 0 1 1 1.50000 6
13000601 0 0 0 1 2.250 1
13000602 0 0 0 1 2.08329 2
13000603 0 0 0 1 2.08333 3
13000604 0 0 0 1 2.45833 4
13000605 0 0 0 1 2.45833 5
13000606 0 0 0 1 1.50000 6
13000701 0 0.0 0.0 0.0 6

```

13000801 0.0 3.0 3.0 0.0 0.0 0.0 0.0 1.0 6
*
*
* thermal shield
*
13150000 8 3 2 1 6.6042
13150100 0 1
13150101 2 6.8333
13150201 5 2
13150301 0.0 2
13150401 530.0 3
13150501 315010000 0 1 1 2.1353 1
13150502 315020000 10000 1 1 2.18328 5
13150503 315060000 0 1 1 2.50627 6
13150504 315070000 0 1 1 1.4590 7
13150505 315080000 0 1 1 3.33328 8
13150601 315010000 0 1 1 2.1353 1
13150602 315020000 10000 1 1 2.18328 5
13150603 315060000 0 1 1 2.50627 6
13150604 315070000 0 1 1 1.4590 7
13150605 315080000 0 1 1 3.33328 8
13150701 0 0.0 0.0 0.0 8
13150801 0.0 3.0 3.0 0.0 0.0 0.0 0.0 1.0 8
13150901 0.0 3.0 3.0 0.0 0.0 0.0 0.0 1.0 8
*
* downcomer vessel wall
*
*
13160000 8 3 2 1 7.2083
13160100 0 1
13160101 2 7.9271
13160201 5 2
13160301 0.0 2
13160401 530.0 3
13160501 315010000 0 1 1 2.1353 1
13160502 315020000 10000 1 1 2.18328 5
13160503 315060000 0 1 1 2.50627 6

13160504 315070000 0 1 1 1.4590 7
 13160505 315080000 0 1 1 3.33328 8
 13160601 0 0 0 1 2.1353 1
 13160602 0 0 0 1 2.18328 5
 13160603 0 0 0 1 2.50627 6
 13160604 0 0 0 1 1.4590 7
 13160605 0 0 0 1 3.33328 8
 13160701 0 0.0 0.0 0.0 8
 13160801 0.0 3.0 3.0 0.0 0.0 0.0 0.0 1.0 8

*

* barrel baffle region - heat slabs between barrel baffle and downcomer

*

13200000 6 3 2 1 6.1667
 13200100 0 1
 13200101 2 6.3542
 13200201 5 2
 13200301 0.0 2
 13200401 530.0 3
 13200501 320010000 0 1 1 2.1353 1
 13200502 320020000 10000 1 1 2.18329 5
 13200503 320060000 0 1 1 2.50627 6
 13200601 315010000 0 1 1 2.1353 1
 13200602 315020000 10000 1 1 2.18329 5
 13200603 315060000 0 1 1 2.50627 6
 13200701 0 0.0 0.0 0.0 6
 13200801 0.0 3.0 3.0 0.0 0.0 0.0 0.0 1.0 6
 13200901 0.0 3.0 3.0 0.0 0.0 0.0 0.0 1.0 6

*

* lower plenum - hemispherical shell, lower plenum wall,

* core barrel wall, internals

*

* hemispherical shell

*

13230000 1 3 3 1 7.35
 13230100 0 1
 13230101 2 7.8136
 13230201 5 2

13230301 0.0 2
13230401 530.0 3
13230501 323010000 0 1 1 0.5 1
13230601 0 0 0 1 0.5 1
13230701 0 0.0 0.0 0.0 1
13230801 0.0 3.0 3.0 0.0 0.0 0.0 0.0 1.0 1

*

* lower plenum wall

*

13220000 1 3 2 1 7.35
13220100 0 1
13220101 2 7.8136
13220201 5 2
13220301 0.0 2
13220401 530.0 3
13220501 322010000 0 1 1 1.81537 1
13220601 0 0 0 1 1.81537 1
13220701 0 0.0 0.0 0.0 1
13220801 0.0 3.0 3.0 0.0 0.0 0.0 0.0 1.0 1

*

* core barrel wall

*

13250000 2 3 2 1 6.1667
13250100 0 1
13250101 2 6.3542
13250201 5 2
13250301 0.0 2
13250401 530.0 3
13250501 325010000 0 1 1 3.33328 1
13250502 330010000 0 1 1 1.4590 2
13250601 315080000 0 1 1 3.33328 1
13250602 315070000 0 1 1 1.4590 2
13250701 0 0.0 0.0 0.0 2
13250801 0.0 3.0 3.0 0.0 0.0 0.0 0.0 1.0 2
13250901 0.0 3.0 3.0 0.0 0.0 0.0 0.0 1.0 2

*

* internals

*

13270000	4	3	1	1	0.0				
13270100	0	1							
13270101	2	0.24944							
13270201	5	2							
13270301	0.0	2							
13270401	530.0	3							
13270501	0	0	0	0	267.4	1			
13270502	0	0	0	0	267.4	2			
13270503	0	0	0	0	493.0	3			
13270504	0	0	0	0	239.0	4			
13270601	323010000	0	1	0	267.4	1			
13270602	322010000	0	1	0	267.4	2			
13270603	325010000	0	1	0	493.0	3			
13270604	330010000	0	1	0	239.0	4			
13270701	0	0.0	0.0	0.0	4				
13270801	0.0	3.0	3.0	0.0	0.0	0.0	0.0	1.0	4
13270901	0.0	3.0	3.0	0.0	0.0	0.0	0.0	1.0	4

*

* core heat slabs - heat slab between core and barrel baffle, fuel pins

*

13350000	6	3	2	1	6.7052				
13350100	0	1							
13350101	2	6.7989							
13350201	5	2							
13350301	0.0	2							
13350401	563.03	1							
13350402	547.21	2							
13350403	540.18	3							
13350501	335010000	0	1	1	2.50627	1			
13350502	335020000	10000	1	1	2.18329	5			
13350503	335060000	0	1	1	2.1353	6			
13350601	320060000	0	1	1	2.50627	1			
13350602	320050000	0	1	1	2.18329	2			
13350603	320040000	0	1	1	2.18329	3			
13350604	320030000	0	1	1	2.18329	4			
13350605	320020000	0	1	1	2.18329	5			

13350606 320010000 0 1 1 2.1353 6
13350701 0 0.0 0.0 0.0 6
13350801 0.0 3.0 3.0 0.0 0.0 0.0 0.0 1.0 6
13350901 0.0 3.0 3.0 0.0 0.0 0.0 0.0 1.0 6
*
* core fuel pin
*
13360000 6 9 2 1 0.0
13360100 0 1
13360101 5 0.014
13360102 1 0.016
13360103 2 0.0165
13360201 1 5
13360202 2 6
13360203 3 8
13360301 1.0 5
13360302 0.0 8
13360401 1100. 3
13360402 900. 6
13360403 620. 7
13360404 570. 9
13360501 0 0 0 0 0.0 1
13360502 0 0 0 0 0.0 2
13360503 0 0 0 0 0.0 3
13360504 0 0 0 0 0.0 4
13360505 0 0 0 0 0.0 5
13360506 0 0 0 0 0.0 6
13360601 335010000 10000 1 0 9497.0473 5
13360602 335060000 0 1 0 4712.2754 6
13360701 1000 0.141211 0.0 0.003769 1
13360702 1000 0.204599 0.0 0.005461 2
13360703 1000 0.208339 0.0 0.005561 3
13360704 1000 0.206780 0.0 0.005520 4
13360705 1000 0.174414 0.0 0.004656 5
13360706 1000 0.038668 0.0 0.001032 6
13360801 0.0 3.0 3.0 0.0 0.0 0.0 0.0 1.0 6
13360901 0.0 3.0 3.0 0.0 0.0 0.0 0.0 1.0 6

*

* upper plenum heat slabs - core barrel , internals

*

* core barrel

*

13500000	6	3	2	1	6.1667				
13500100	0	1							
13500101	2	6.3542							
13500201	5	2							
13500301	0.0	2							
13500401	530.0	2							
13500402	530.0	3							
13500501	340010000	0	1	1	2.24999	1			
13500502	345010000	0	1	1	2.08329	2			
13500503	350040000	0	1	1	2.08333	3			
13500504	350030000	0	1	1	2.45833	4			
13500505	350020000	0	1	1	2.45833	5			
13500506	350010000	0	1	1	1.49999	6			
13500601	305010000	0	1	1	2.24999	1			
13500602	300010000	0	1	1	2.08329	2			
13500603	310010000	0	1	1	2.08333	3			
13500604	310020000	0	1	1	2.45833	4			
13500605	310030000	0	1	1	2.45833	5			
13500606	310040000	0	1	1	1.49999	6			
13500701	0	0.0	0.0	0.0	6				
13500801	0.0	3.0	3.0	0.0	0.0	0.0	0.0	1.0	6
13500901	0.0	3.0	3.0	0.0	0.0	0.0	0.0	1.0	6

*

* internals

*

13510000	6	3	1	1	0.0				
13510100	0	1							
13510101	2	0.0495							
13510201	5	2							
13510301	0.0	2							
13510401	530.0	3							
13510501	0	0	0	0	775.1	1			

13510502 0 0 0 0 521.00 3
 13510503 0 0 0 0 667.333 6
 13510601 340010000 0 1 0 775.1 1
 13510602 345010000 0 1 0 521.00 3
 13510603 350010000 0 1 0 667.333 6
 13510701 0 0.0 0.0 0.0 6
 13510801 0.0 3.0 3.0 0.0 0.0 0.0 0.0 1.0 6
 13510901 0.0 3.0 3.0 0.0 0.0 0.0 0.0 1.0 6

*

* upper head - hemisphere shell ,vessel wall, internals

*

* hemispherical shell

*

13550000 1 3 3 1 7.1443
 13550100 0 1
 13550101 2 7.7657
 13550201 5 2
 13550301 0.0 2
 13550401 530.00 3
 13550501 356010000 0 1 1 0.5 1
 13550601 0 0 0 1 0.5 1
 13550701 0 0.0 0.0 0.0 1
 13550801 0.0 3.0 3.0 0.0 0.0 0.0 0.0 1.0 1
 13550901 0.0 3.0 3.0 0.0 0.0 0.0 0.0 1.0 1

*

* vessel wall

*

13570000 2 3 2 1 7.1443
 13570100 0 1
 13570101 2 7.7657
 13570201 5 2
 13570301 0.0 2
 13570401 530.0 3
 13570501 356020000 10000 1 1 1.3485 2
 13570601 0 0 0 1 1.3485 1
 13570602 0 0 0 1 1.3485 2
 13570701 0 0.0 0.0 0.0 2

13570801 0.0 3.0 3.0 0.0 0.0 0.0 0.0 1.0 2
*
* internals
*
13560000 4 3 1 1 0.0
13560100 0 1
13560101 2 0.472
13560201 5 2
13560301 0.0 2
13560401 530.00 3
13560501 0 0 0 0 125.325 1
13560502 0 0 0 0 125.325 2
13560503 0 0 0 0 125.325 3
13560504 0 0 0 0 125.325 4
13560601 355010000 0 1 0 125.325 1
13560602 356030000 -10000 1 0 125.325 4
13560701 0 0.0 0.0 0.0 4
13560801 0.0 3.0 3.0 0.0 0.0 0.0 0.0 1.0 4
13560901 0.0 3.0 3.0 0.0 0.0 0.0 0.0 1.0 4
*
20100100 tbl/fctn 1 1 * core fuel
20100200 tbl/fctn 1 1 * core fuel gap
20100300 tbl/fctn 1 1 * core fuel cladding
20100400 tbl/fctn 1 1 * inconel
20100500 tbl/fctn 1 1 * stainless steel
* *
*
20100101 32.0 2.284e-3 188.6 2.284e-3
20100102 332.6 2.1235e-3
20100103 440.6 8.951e-4
20100104 500.0 8.2806e-04
20100105 650.0 6.4194e-04
20100106 800.0 5.4361e-04
20100107 950.0 5.7750e-04
20100108 1100.0 4.2278e-04
20100109 1250.0 7.7722e-04
20100110 1400.0 7.3889e-04

20100111	1500.0	8.0739e-04
20100112	1700.0	8.7789e-04
20100113	1850.0	4.5628e-04
20100114	2000.0	3.3556e-04
20100115	2150.0	5.1661e-04
20100116	2300.0	4.0472e-04
20100117	2450.0	3.5306e-04
20100118	2600.0	6.6689e-04
20100119	3100.0	5.4350e-04
20100120	3600.0	3.7228e-04
20100121	4100.0	4.6156e-04
20100122	4600.0	5.4722e-04
20100123	5100.0	2.3056e-04
*		
*		
20100151	32.0	30.45
20100152	122.0	34.35
20100153	212.0	47.75
20100154	392.0	44.55
20100155	752.0	45.70
20100156	2012.0	41.35
20100157	2732.0	32.65
20100158	3092.0	66.55
20100159	3452.0	83.05
20100160	3812.0	52.80
20100161	4352.0	69.70
20100162	4532.0	44.25
20100163	4712.0	38.15
20100164	4892.0	120.10
20100165	5144.0	96.40
20100166	8000.0	131.40
*		
20100201	32.0	2.4487788e-04
20100202	5400.0	2.4487788e-04
*		
*		
20100251	32.0	0.000065

20100252	5400.0	0.000065		
*				
*				
*				
20100301	32.0	2.9267e-03	392.0	2.9267e-03
20100302	752.0	1.2478e-03		
20100303	1112.0	4.7297e-03		
20100304	1472.0	5.0508e-03		
20100305	1832.0	6.5325e-03		
20100306	2192.0	4.0142e-03		
20100307	2552.0	5.8169e-03		
20100308	2912.0	8.7803e-03		
20100309	3272.0	1.0647e-03		
20100310	3632.0	1.8311e-03		
20100311	3992.0	9.0918e-02		
*				
*				
20100351	0.0	26.392		
20100352	1480.3	35.476		
20100353	1675.0	75.176		
20100354	1787.5	44.370		
20100355	3500.0	24.476		
*				
*				
20100401	32.0	2.1167e-03		
20100402	1050.0	4.0394e-03		
*				
*				
20100451	32.0	57.180	100.0	57.180
20100452	400.0	61.140		
20100453	600.0	63.770		
20100454	800.0	66.410		
*				
*				
*				
20100501	32.0	2.0833e-03		
20100502	1700.0	4.0294e-03		

```

*
*
20100551  32.0  57.114  200.0  57.114
20100552  300.0  59.118
20100553  400.0  61.122
20100554  500.0  63.126
20100555  600.0  64.629
20100556  700.0  66.130
20100557  800.0  67.134
20100558  1000.0  69.138
20100559  2000.0  80.160
*

```

```

*
*
20200200  reac-t      503  1.0 -20.65
*          time (sec)  reactivity ($)
20200201  -1.0      0.0
20200202   0.0      0.0
20200203   0.7      0.0
20200204   0.9      0.02
20200205   1.4      0.13
20200206   1.9      0.33
20200207   2.4      0.70
20200208   2.9      0.96
20200209   3.1      1.00
20200210  1.0+6      1.00
*

```

* end of input deck - problem end *

```

20500100  cormass  sum  0.0624306  0.0  1
****   a0  ai  alp(i)  volno(i)  ai  alph(i)  volno(i)
20500101  0.0  133.85  rho  335010000  116.60  rho  335020000
20500102  116.60  rho  335030000  116.60  rho  335040000
20500103  116.60  rho  335050000  114.04  rho  335060000
20500200  upmass  sum  0.0624306  0.0  1

```

20500201 0.0 254.25 rho 340010000 235.41 rho 345010000
 20500202 135.35 rho 350010000 277.79 rho 350020000
 20500203 277.79 rho 350030000 235.41 rho 350040000
 20500300 lpmass sum 0.0624306 0.0 1
 20500301 0.0 236.00 rho 322010000 236.00 rho 323010000
 20500302 304.00 rho 325010000 164.00 rho 330010000
 20500400 dnmass sum 0.0624306 0.0 1
 20500401 0.0 57.056 rho 315010000 58.338 rho 315020000
 20500402 58.338 rho 315030000 58.338 rho 315040000
 20500403 58.338 rho 315050000 66.968 rho 315060000
 20500404 38.987 rho 315070000 89.065 rho 315080000
 20500405 66.042 rho 305010000 41.239 rho 300010000
 20500406 41.239 rho 310010000 80.244 rho 310020000
 20500407 38.054 rho 310030000 22.635 rho 310040000
 20500408 39.874 rho 320010000 40.770 rho 320020000
 20500409 40.770 rho 320030000 40.770 rho 320040000
 20500410 40.770 rho 320050000 46.802 rho 320060000
 20500500 uhmass sum 0.0624306 0.0 1
 20500501 0.0 122.25 rho 355010000 122.25 rho 356010000
 20500502 122.25 rho 356020000 122.25 rho 356030000
 20500800 iclpsmss sum 0.0624306 0.0 1
 20500801 0.0 72.342 rho 112010000 74.967 rho 112020000
 20500802 105.49 rho 112030000 66.335 rho 112040000
 20500803 109.09 rho 112050000
 20500900 iclpmss sum 0.0624306 0.0 1
 20500901 0.0 168.00 rho 113010000 93.000 rho 114010000
 20500902 93.289 rho 116010000 93.289 rho 118010000
 20500903 75.750 rho 118020000
 20501700 vesmass sum 1.0 0.0 1
 20501701 0.0 1.0 cntrlvar 1 1.0 cntrlvar 2
 20501702 1.0 cntrlvar 3 1.0 cntrlvar 4
 20501703 1.0 cntrlvar 5
 20502100 corlev sum 0.018724 0.0 1
 20502101 714.29 -133.85 voidg 335010000 -116.60 voidg 335020000
 20502102 -116.60 voidg 335030000 -116.60 voidg 335040000
 20502103 -116.60 voidg 335050000 -114.04 voidg 335060000
 §*****

\$ space independent reactor kinetics data

30000000 point

30000001 gamma-ac 3600.e6 0.0 297.0 1.0 0.48

30000002 ans79-1

30000011 2

30000501 45.0 0.0

30000601 1600.0 0.0

30000701 335010000 0 0.1109 0.

30000702 335020000 0 0.2327 0.

30000703 335030000 0 0.2413 0.

30000704 335040000 0 0.2377 0.

30000705 335050000 0 0.1691 0.

30000706 335060000 0 0.0083 0.

30000801 3360001 0 0.1109 0.

30000802 3360002 0 0.2327 0.

30000803 3360003 0 0.2413 0.

30000804 3360004 0 0.2377 0.

30000805 3360005 0 0.1691 0.

30000806 3360006 0 0.0083 0.

ORIGEN-ARP Data & Results

20GWd/MTU Total Decay Heat by Isotope

Case 5

time (h)

total power (watts)

nuclide

13 41

1.000E-03 3.000E-03 1.000E-02 3.000E-02 1.000E-01 3.000E-01 5.000E-01
1.500E+00 4.500E+00 1.350E+01 2.400E+01 3.000E+01 7.200E+01

la140 1.314E+06 1.314E+06 1.314E+06 1.314E+06 1.314E+06 1.313E+06 1.313E+06
1.312E+06 1.308E+06 1.295E+06 1.277E+06 1.266E+06 1.180E+06

np239 1.873E+06 1.873E+06 1.873E+06 1.873E+06 1.873E+06 1.872E+06 1.870E+06
1.851E+06 1.785E+06 1.599E+06 1.406E+06 1.306E+06 7.802E+05

i132 9.350E+05 9.350E+05 9.350E+05 9.349E+05 9.348E+05 9.342E+05 9.335E+05
9.290E+05 9.094E+05 8.414E+05 7.667E+05 7.269E+05 5.010E+05

zr95 3.713E+05 3.713E+05 3.713E+05 3.713E+05 3.713E+05 3.713E+05 3.713E+05
3.711E+05 3.706E+05 3.691E+05 3.674E+05 3.664E+05 3.595E+05

nb95 3.478E+05 3.478E+05 3.478E+05 3.478E+05 3.478E+05 3.478E+05 3.478E+05
3.478E+05 3.478E+05 3.479E+05 3.479E+05 3.479E+05 3.478E+05

pr144 2.781E+05 2.781E+05 2.780E+05 2.780E+05 2.778E+05 2.773E+05 2.771E+05
2.767E+05 2.767E+05 2.763E+05 2.760E+05 2.758E+05 2.746E+05

y91 2.214E+05 2.214E+05 2.214E+05 2.214E+05 2.214E+05 2.214E+05 2.214E+05
2.214E+05 2.213E+05 2.209E+05 2.200E+05 2.195E+05 2.151E+05

mo99 3.030E+05 3.030E+05 3.030E+05 3.030E+05 3.028E+05 3.022E+05
3.015E+05 2.984E+05 2.891E+05 2.630E+05 2.355E+05 2.211E+05 1.422E+05

ba140 2.159E+05 2.159E+05 2.159E+05 2.159E+05 2.159E+05 2.158E+05 2.157E+05
2.152E+05 2.137E+05 2.094E+05 2.045E+05 2.017E+05 1.834E+05

sr89 1.692E+05 1.692E+05 1.692E+05 1.692E+05 1.692E+05 1.692E+05 1.692E+05
1.691E+05 1.688E+05 1.679E+05 1.669E+05 1.664E+05 1.624E+05

ru103 1.666E+05 1.666E+05 1.666E+05 1.666E+05 1.666E+05 1.666E+05 1.665E+05
1.664E+05 1.660E+05 1.650E+05 1.637E+05 1.630E+05 1.580E+05

i133 5.035E+05 5.035E+05 5.035E+05 5.035E+05 5.033E+05 5.023E+05 5.007E+05
4.888E+05 4.454E+05 3.303E+05 2.328E+05 1.906E+05 4.702E+04

ce143 2.847E+05 2.847E+05 2.847E+05 2.847E+05 2.846E+05 2.841E+05 2.833E+05
2.779E+05 2.609E+05 2.160E+05 1.732E+05 1.527E+05 6.321E+04

pr143 1.223E+05 1.223E+05 1.223E+05 1.223E+05 1.223E+05 1.223E+05 1.223E+05
1.223E+05 1.223E+05 1.220E+05 1.212E+05 1.205E+05 1.141E+05

i131 1.298E+05 1.298E+05 1.298E+05 1.298E+05 1.298E+05 1.298E+05 1.298E+05
1.296E+05 1.285E+05 1.250E+05 1.210E+05 1.186E+05 1.030E+05

nb97 4.853E+05 4.853E+05 4.853E+05 4.853E+05 4.852E+05 4.843E+05 4.831E+05
4.732E+05 4.282E+05 2.983E+05 1.940E+05 1.515E+05 2.533E+04

ce141 1.019E+05 1.019E+05 1.019E+05 1.019E+05 1.019E+05 1.019E+05 1.019E+05
1.019E+05 1.018E+05 1.012E+05 1.003E+05 9.979E+04 9.614E+04

zr97 3.774E+05 3.774E+05 3.773E+05 3.770E+05 3.759E+05 3.728E+05 3.698E+05
3.549E+05 3.138E+05 2.170E+05 1.410E+05 1.103E+05 1.969E+04

te132 1.106E+05 1.106E+05 1.106E+05 1.106E+05 1.105E+05 1.104E+05 1.102E+05
1.092E+05 1.063E+05 9.818E+04 8.946E+04 8.482E+04 5.845E+04

xe133 8.605E+04 8.605E+04 8.605E+04 8.605E+04 8.605E+04 8.605E+04 8.606E+04
8.607E+04 8.604E+04 8.525E+04 8.332E+04 8.189E+04 6.896E+04

nb97m 3.002E+05 3.002E+05 3.001E+05 2.999E+05 2.990E+05 2.967E+05
2.943E+05 2.824E+05 2.497E+05 1.726E+05 1.122E+05 8.773E+04 1.567E+04

rh106 7.287E+04 7.167E+04 6.876E+04 6.579E+04 6.510E+04 6.510E+04 6.510E+04
6.510E+04 6.508E+04 6.503E+04 6.498E+04 6.495E+04 6.474E+04

nd147 6.585E+04 6.585E+04 6.585E+04 6.585E+04 6.585E+04 6.583E+04 6.581E+04
 6.565E+04 6.514E+04 6.361E+04 6.188E+04 6.091E+04 5.454E+04
 tc99m 6.239E+04 6.239E+04 6.239E+04 6.239E+04 6.239E+04 6.238E+04 6.238E+04
 6.230E+04 6.172E+04 5.818E+04 5.288E+04 4.981E+04 3.215E+04
 y93 5.184E+05 5.184E+05 5.184E+05 5.183E+05 5.175E+05 5.129E+05 5.067E+05
 4.734E+05 3.853E+05 2.078E+05 1.011E+05 6.696E+04 3.750E+03
 sr91 4.837E+05 4.837E+05 4.837E+05 4.833E+05 4.810E+05 4.741E+05 4.672E+05
 4.344E+05 3.492E+05 1.813E+05 8.442E+04 5.454E+04 2.563E+03
 xe135 1.007E+05 1.008E+05 1.009E+05 1.011E+05 1.020E+05 1.045E+05 1.068E+05
 1.165E+05 1.320E+05 1.166E+05 7.225E+04 5.141E+04 2.968E+03
 te131m 6.369E+04 6.369E+04 6.369E+04 6.367E+04 6.359E+04 6.337E+04
 6.312E+04 6.177E+04 5.765E+04 4.683E+04 3.674E+04 3.198E+04 1.212E+04
 ce144 2.467E+04 2.467E+04 2.467E+04 2.467E+04 2.467E+04 2.467E+04 2.467E+04
 2.467E+04 2.466E+04 2.464E+04 2.461E+04 2.460E+04 2.449E+04
 pm149 3.552E+04 3.552E+04 3.552E+04 3.552E+04 3.551E+04 3.550E+04
 3.548E+04 3.530E+04 3.434E+04 3.069E+04 2.676E+04 2.474E+04 1.430E+04
 rh105 3.657E+04 3.657E+04 3.657E+04 3.657E+04 3.657E+04 3.658E+04 3.658E+04
 3.652E+04 3.586E+04 3.173E+04 2.625E+04 2.340E+04 1.030E+04
 i135 9.077E+05 9.075E+05 9.070E+05 9.052E+05 8.986E+05 8.798E+05 8.614E+05
 7.752E+05 5.649E+05 2.186E+05 7.219E+04 3.833E+04 4.562E+02
 u237 1.915E+04 1.915E+04 1.915E+04 1.915E+04 1.914E+04 1.912E+04 1.911E+04
 1.903E+04 1.878E+04 1.807E+04 1.728E+04 1.684E+04 1.407E+04
 pm148 1.862E+04 1.862E+04 1.862E+04 1.862E+04 1.861E+04 1.859E+04
 1.858E+04 1.848E+04 1.819E+04 1.734E+04 1.640E+04 1.589E+04 1.272E+04
 eu156 1.463E+04 1.463E+04 1.463E+04 1.463E+04 1.463E+04 1.462E+04 1.462E+04
 1.460E+04 1.454E+04 1.435E+04 1.409E+04 1.394E+04 1.288E+04
 sb127 1.670E+04 1.670E+04 1.670E+04 1.670E+04 1.670E+04 1.669E+04 1.667E+04
 1.660E+04 1.632E+04 1.530E+04 1.414E+04 1.352E+04 9.867E+03
 rh103m 1.125E+04 1.125E+04 1.125E+04 1.125E+04 1.124E+04 1.124E+04
 1.124E+04 1.123E+04 1.121E+04 1.114E+04 1.106E+04 1.100E+04 1.067E+04
 pm151 2.341E+04 2.341E+04 2.341E+04 2.340E+04 2.340E+04 2.334E+04
 2.326E+04 2.273E+04 2.113E+04 1.696E+04 1.312E+04 1.134E+04 4.066E+03
 y91m 1.157E+05 1.157E+05 1.157E+05 1.157E+05 1.156E+05 1.154E+05
 1.150E+05 1.106E+05 9.118E+04 4.753E+04 2.211E+04 1.428E+04 6.710E+02
 pm148m 8.868E+03 8.868E+03 8.868E+03 8.868E+03 8.867E+03 8.866E+03
 8.865E+03 8.858E+03 8.840E+03 8.784E+03 8.720E+03 8.684E+03 8.432E+03
 total 7.793E+07 6.724E+07 5.554E+07 4.542E+07 3.609E+07 2.831E+07 2.453E+07
 1.726E+07 1.243E+07 9.138E+06 7.679E+06 7.156E+06 5.273E+06

20GWd/MTU Iodine-135 & Xenon-135 Densities

Case 5

time (h)

grams / cubic centimeter

nuclide

13 3

	1.000E-03	3.000E-03	1.000E-02	3.000E-02	1.000E-01	3.000E-01	5.000E-01
	1.500E+00	4.500E+00	1.350E+01	2.400E+01	3.000E+01	7.200E+01	
i135	2.038E-04	2.038E-04	2.036E-04	2.032E-04	2.017E-04	1.975E-04	1.934E-04
	1.740E-04	1.268E-04	4.907E-05	1.621E-05	8.606E-06	1.024E-07	
xe135	1.083E-04	1.083E-04	1.084E-04	1.087E-04	1.097E-04	1.123E-04	1.148E-04
	1.253E-04	1.420E-04	1.253E-04	7.768E-05	5.527E-05	3.191E-06	
total	5.170E+00	5.170E+00	5.170E+00	5.170E+00	5.170E+00	5.170E+00	5.170E+00
	5.170E+00	5.170E+00	5.170E+00	5.170E+00	5.170E+00	5.170E+00	5.170E+00

30 GWd/MTU Total Decay Heat by Isotope

Case 5

time (h)

total power (watts)

nuclide

13 41

	1.000E-03	3.000E-03	1.000E-02	3.000E-02	1.000E-01	3.000E-01	5.000E-01
	1.500E+00	4.500E+00	1.350E+01	2.400E+01	3.000E+01	7.200E+01	
la140	1.313E+06	1.313E+06	1.313E+06	1.313E+06	1.313E+06	1.313E+06	1.313E+06
	1.312E+06	1.307E+06	1.294E+06	1.277E+06	1.266E+06	1.180E+06	
np239	1.882E+06	1.882E+06	1.882E+06	1.882E+06	1.882E+06	1.881E+06	1.878E+06
	1.860E+06	1.794E+06	1.606E+06	1.412E+06	1.312E+06	7.840E+05	
i132	9.352E+05	9.352E+05	9.352E+05	9.351E+05	9.350E+05	9.344E+05	9.337E+05
	9.292E+05	9.096E+05	8.415E+05	7.668E+05	7.271E+05	5.010E+05	
zr95	3.711E+05	3.711E+05	3.711E+05	3.711E+05	3.711E+05	3.711E+05	3.711E+05
	3.709E+05	3.704E+05	3.689E+05	3.672E+05	3.662E+05	3.593E+05	
nb95	3.476E+05	3.476E+05	3.476E+05	3.476E+05	3.476E+05	3.476E+05	3.476E+05
	3.476E+05	3.477E+05	3.477E+05	3.477E+05	3.477E+05	3.476E+05	
pr144	2.779E+05	2.779E+05	2.779E+05	2.778E+05	2.776E+05	2.772E+05	2.769E+05
	2.765E+05	2.766E+05	2.761E+05	2.758E+05	2.757E+05	2.745E+05	

y91 2.212E+05 2.212E+05 2.212E+05 2.212E+05 2.212E+05 2.212E+05 2.212E+05 2.212E+05
2.212E+05 2.211E+05 2.207E+05 2.198E+05 2.193E+05 2.149E+05

mo99 3.030E+05 3.030E+05 3.030E+05 3.029E+05 3.027E+05 3.021E+05
3.015E+05 2.983E+05 2.891E+05 2.630E+05 2.355E+05 2.211E+05 1.422E+05

ba140 2.158E+05 2.158E+05 2.158E+05 2.158E+05 2.158E+05 2.157E+05 2.156E+05
2.151E+05 2.137E+05 2.094E+05 2.044E+05 2.017E+05 1.834E+05

sr89 1.690E+05 1.690E+05 1.690E+05 1.690E+05 1.690E+05 1.690E+05 1.690E+05
1.689E+05 1.686E+05 1.677E+05 1.667E+05 1.662E+05 1.622E+05

ru103 1.668E+05 1.668E+05 1.668E+05 1.668E+05 1.668E+05 1.668E+05 1.667E+05
1.666E+05 1.662E+05 1.652E+05 1.639E+05 1.632E+05 1.582E+05

i133 5.035E+05 5.035E+05 5.035E+05 5.035E+05 5.033E+05 5.023E+05 5.007E+05
4.888E+05 4.454E+05 3.303E+05 2.328E+05 1.906E+05 4.702E+04

ce143 2.846E+05 2.846E+05 2.846E+05 2.846E+05 2.845E+05 2.840E+05 2.832E+05
2.777E+05 2.608E+05 2.159E+05 1.731E+05 1.526E+05 6.317E+04

pr143 1.222E+05 1.222E+05 1.222E+05 1.222E+05 1.222E+05 1.222E+05 1.222E+05
1.222E+05 1.222E+05 1.219E+05 1.211E+05 1.205E+05 1.140E+05

i131 1.299E+05 1.299E+05 1.299E+05 1.299E+05 1.299E+05 1.299E+05 1.298E+05
1.296E+05 1.286E+05 1.251E+05 1.210E+05 1.187E+05 1.031E+05

nb97 4.852E+05 4.852E+05 4.852E+05 4.852E+05 4.851E+05 4.842E+05 4.830E+05
4.731E+05 4.281E+05 2.983E+05 1.940E+05 1.515E+05 2.533E+04

ce141 1.019E+05 1.019E+05 1.019E+05 1.019E+05 1.019E+05 1.019E+05 1.019E+05
1.019E+05 1.018E+05 1.012E+05 1.003E+05 9.976E+04 9.611E+04

zr97 3.773E+05 3.773E+05 3.772E+05 3.769E+05 3.758E+05 3.727E+05 3.697E+05
3.548E+05 3.137E+05 2.169E+05 1.410E+05 1.102E+05 1.969E+04

te132 1.106E+05 1.106E+05 1.106E+05 1.106E+05 1.106E+05 1.104E+05 1.102E+05
1.092E+05 1.064E+05 9.820E+04 8.947E+04 8.484E+04 5.846E+04

xe133 8.604E+04 8.604E+04 8.604E+04 8.604E+04 8.604E+04 8.605E+04 8.605E+04
8.607E+04 8.603E+04 8.524E+04 8.332E+04 8.188E+04 6.896E+04

nb97m 3.002E+05 3.001E+05 3.001E+05 2.998E+05 2.990E+05 2.966E+05
2.942E+05 2.823E+05 2.496E+05 1.726E+05 1.122E+05 8.771E+04 1.566E+04

rh106 7.310E+04 7.190E+04 6.898E+04 6.601E+04 6.533E+04 6.533E+04 6.533E+04
6.532E+04 6.531E+04 6.526E+04 6.521E+04 6.518E+04 6.496E+04

nd147 6.584E+04 6.584E+04 6.584E+04 6.584E+04 6.584E+04 6.582E+04 6.580E+04
6.564E+04 6.512E+04 6.360E+04 6.187E+04 6.090E+04 5.453E+04

tc99m 6.238E+04 6.238E+04 6.238E+04 6.238E+04 6.238E+04 6.238E+04 6.237E+04
6.229E+04 6.171E+04 5.818E+04 5.287E+04 4.981E+04 3.215E+04

y93 5.180E+05 5.180E+05 5.180E+05 5.179E+05 5.172E+05 5.125E+05 5.063E+05
4.731E+05 3.851E+05 2.076E+05 1.010E+05 6.691E+04 3.747E+03

sr91 4.832E+05 4.832E+05 4.832E+05 4.828E+05 4.806E+05 4.736E+05 4.668E+05
 4.340E+05 3.488E+05 1.812E+05 8.434E+04 5.449E+04 2.560E+03
 xe135 1.011E+05 1.011E+05 1.012E+05 1.015E+05 1.024E+05 1.049E+05 1.072E+05
 1.169E+05 1.323E+05 1.167E+05 7.231E+04 5.144E+04 2.969E+03
 te131m 6.375E+04 6.374E+04 6.374E+04 6.372E+04 6.364E+04 6.342E+04
 6.317E+04 6.182E+04 5.770E+04 4.686E+04 3.677E+04 3.201E+04 1.213E+04
 ce144 2.466E+04 2.466E+04 2.466E+04 2.466E+04 2.466E+04 2.466E+04 2.466E+04
 2.465E+04 2.465E+04 2.462E+04 2.460E+04 2.458E+04 2.448E+04
 pm149 3.554E+04 3.554E+04 3.554E+04 3.554E+04 3.554E+04 3.552E+04
 3.550E+04 3.533E+04 3.437E+04 3.071E+04 2.678E+04 2.476E+04 1.431E+04
 rh105 3.667E+04 3.667E+04 3.667E+04 3.667E+04 3.667E+04 3.668E+04 3.668E+04
 3.663E+04 3.596E+04 3.182E+04 2.633E+04 2.347E+04 1.032E+04
 i135 9.077E+05 9.075E+05 9.070E+05 9.052E+05 8.986E+05 8.798E+05 8.614E+05
 7.752E+05 5.649E+05 2.186E+05 7.219E+04 3.833E+04 4.562E+02
 u237 1.930E+04 1.930E+04 1.930E+04 1.930E+04 1.929E+04 1.928E+04 1.926E+04
 1.918E+04 1.893E+04 1.822E+04 1.742E+04 1.698E+04 1.418E+04
 pm148 1.870E+04 1.870E+04 1.869E+04 1.869E+04 1.869E+04 1.867E+04
 1.865E+04 1.855E+04 1.825E+04 1.740E+04 1.646E+04 1.595E+04 1.277E+04
 eu156 1.468E+04 1.468E+04 1.468E+04 1.468E+04 1.467E+04 1.467E+04 1.467E+04
 1.465E+04 1.459E+04 1.439E+04 1.414E+04 1.398E+04 1.293E+04
 sb127 1.672E+04 1.672E+04 1.672E+04 1.672E+04 1.672E+04 1.671E+04 1.669E+04
 1.662E+04 1.634E+04 1.532E+04 1.416E+04 1.354E+04 9.879E+03
 rh103m 1.126E+04 1.126E+04 1.126E+04 1.126E+04 1.126E+04 1.126E+04
 1.126E+04 1.125E+04 1.122E+04 1.115E+04 1.107E+04 1.102E+04 1.068E+04
 pm151 2.343E+04 2.343E+04 2.343E+04 2.343E+04 2.342E+04 2.337E+04
 2.328E+04 2.275E+04 2.115E+04 1.698E+04 1.314E+04 1.135E+04 4.070E+03
 y91m 1.155E+05 1.155E+05 1.155E+05 1.155E+05 1.155E+05 1.153E+05
 1.148E+05 1.104E+05 9.109E+04 4.748E+04 2.209E+04 1.427E+04 6.703E+02
 pm148m 8.931E+03 8.931E+03 8.931E+03 8.930E+03 8.930E+03 8.929E+03
 8.928E+03 8.921E+03 8.903E+03 8.847E+03 8.782E+03 8.745E+03 8.492E+03
 total 7.794E+07 6.725E+07 5.555E+07 4.543E+07 3.610E+07 2.832E+07 2.454E+07
 1.727E+07 1.244E+07 9.145E+06 7.686E+06 7.162E+06 5.276E+06

20GWd/MTU Iodine-135 & Xenon-135 Densities

Case 5

time (h)

grams / cubic centimeter

nuclide

13 3

	1.000E-03	3.000E-03	1.000E-02	3.000E-02	1.000E-01	3.000E-01	5.000E-01
	1.500E+00	4.500E+00	1.350E+01	2.400E+01	3.000E+01	7.200E+01	
i135	2.038E-04	2.038E-04	2.036E-04	2.032E-04	2.017E-04	1.975E-04	1.934E-04
	1.740E-04	1.268E-04	4.907E-05	1.621E-05	8.606E-06	1.024E-07	
xe135	1.087E-04	1.087E-04	1.088E-04	1.091E-04	1.101E-04	1.127E-04	1.152E-04
	1.256E-04	1.422E-04	1.255E-04	7.774E-05	5.531E-05	3.193E-06	
total	9.927E+02	9.927E+02	9.927E+02	9.927E+02	9.927E+02	9.927E+02	9.927E+02
	9.927E+02	9.927E+02	9.927E+02	9.927E+02	9.927E+02	9.927E+02	9.927E+02